


Physiological roles of the chloroplast acetyltransferase
GNAT1 and GNAT2 in *Arabidopsis thaliana*

Master's thesis
University of Turku
Department of Life Technologies
Biosciences
Molecular Systems Biology
June 2024



Shahnawaz Ami

The originality of this thesis has been checked in accordance with the University of Turku quality assurance system using the Turnitin OriginalityCheck service.

UNIVERSITY OF TURKU

Department of Life Technologies

SHAHNAWAZ AMI: Physiological roles of the chloroplast acetyltransferase GNAT1 and GNAT2 in *Arabidopsis thaliana*

Master's thesis, 73 p.,

Biosciences

Molecular Systems Biology

June 2024

The originality of this thesis has been checked in accordance with the University of Turku quality assurance system using the Turnitin OriginalityCheck service

The acetylation machinery in the chloroplast consists of eight acetyltransferase enzymes that belong to the General control non-repressible 5-related N-acetyltransferase (GNAT) superfamily. Loss of the GNAT2 enzyme has been shown to affect regulation of photosynthetic light harvesting, thylakoid dynamics, plant phenotype and acetylation level of chloroplast proteins, but the detailed effects on seed germination, root development, thylakoid protein acetylation and *de novo* synthesis of Photosystem II (PSII), are yet to be studied. Therefore, the aims of my thesis are (i) to understand the effect of GNAT2 on thylakoid protein accumulation and acetylation of light-harvesting complex II (LHCII) proteins; (ii) to assess the germination and root morphology of wild-type (WT) and *gnat2* knock-out mutant under standard conditions and osmotic stress; (iii) to understand the role of GNAT1 and GNAT1/2 in the early stages of PSII biosynthesis in *Arabidopsis thaliana*.

For the analysis of GNAT2's effect on thylakoid protein accumulation, proteins extracted from five weeks old WT and *gnat2* plants were separated by 2D sodium dodecyl sulfate polyacrylamide gel electrophoresis (SDS-PAGE) and analysed by liquid chromatography electrospray ionization tandem mass spectrometry (LC-ESI-MS/MS). For the assessment of germination and root morphology, WT and *gnat2* plants were grown on ½ Murashige Skoog (MS) media under standard and osmotic stress condition induced by 200 mM mannitol. For assessing GNAT1 & GNAT2's role in PSII biosynthesis, proteins extracted from two weeks old WT, *gnat1* and *gnat2* plants were subjected to clear native polyacrylamide gel electrophoresis (CN-PAGE).

The results obtained indicate that the loss of GNAT2 led to decreased seed germination and overall decrease in root growth under both conditions. Separation of thylakoid proteins by 2D SDS-PAGE followed by LC-MS/MS analysis of revealed that the acetylation level of LHCB 1 and LHCB 2 were clearly decreased in the *gnat2* mutant. The analysis of PSII assembly indicated differences in the accumulation of PSII-LHCII supercomplexes and LHCII assembly complex. Overall, the study has potential to bring in new insights into the physiological role(s) of chloroplast protein acetylation.

Keywords: acetylation, acetyltransferase, *Arabidopsis*, chloroplast, light harvesting protein, Photosystem II, root morphology

Contents

1. Introduction	3
1.1 Protein acetylation.....	3
1.1.1 N-terminal acetylation.....	4
1.1.2 Lys acetylation.....	6
1.2 Chloroplast acetyltransferases.....	8
1.3 GNAT2 and its effect on physiology.....	9
1.4 Photosynthesis.....	11
1.4.1 Photosystems and LHC complexes.....	11
1.4.2 Photosynthetic electron transfer.....	12
1.4.3 Carbon assimilation.....	13
1.4.4 PSII structure and biosynthesis.....	13
1.5 <i>Arabidopsis thaliana</i>	14
2. Aims of the study	15
3. Materials and Methods	16
3.1 Plant materials and growth conditions.....	16
3.2 Root development and germination test.....	16
3.3 Isolation of thylakoids.....	16
3.4 Chlorophyll concentration determination.....	17
3.5 2D gel electrophoresis.....	17
3.5.1 IEF and SDS-PAGE.....	17
3.5.2. Gel imaging.....	17
3.5.3 Digestion and LC-ESI-MS/MS analysis.....	18
3.6 CN-PAGE.....	18
3.6.1 Gel preparation.....	18
3.6.2. Sample preparation, run and imaging.....	19
3.7 Statistical analysis.....	19
3.8 Artificial Intelligence disclaimer.....	19
4. Results	20
4.1 Germination and root growth in WT and gnat2 plants.....	20
4.2. 2D gel electrophoresis of WT and gnat2 thylakoid complexes.....	24
4.3. CN-PAGE of intact WT, gnat1 and gnat2 thylakoid complexes.....	35
5. Discussion	37
5.1 The GNAT2 enzyme affects the acetylation level of the LHCB proteins.....	37
5.2 The loss of the GNAT2 enzyme results in defects in seed germination and growth of roots under standard and osmotic stress conditions.....	38
5.3 Both GNAT1 and GNAT2 may affect the accumulation of thylakoid protein complexes.....	40
6. Conclusion	42
7. References	43

Abbreviation

Acetyl-CoA	Ac-CoA
Ac-CoA-citrate lyase	ACL
Ac-CoA synthetase	AceSC
Adenosine triphosphate	ATP
Beta-dodecylmaltoside	β -DM
Clear Native	CN
Dithiothreitol	DTT
Electrospray ionization	ESI
General control non-repressible	
5 (GCN5)-related N-acetyltransferase	GNAT
Global Acetylation Profiling	GAP
Green fluorescent protein	GFP
Histone acetyltransferases	HAT
Initiation methionine	iMet
Isoelectric focusing	IEF
Isoelectric point	pI
Light harvesting complex	LHC
Liquid chromatography	LC
Lysine acetyltransferase	KAT
Lysine deacetylase	KDAC
Mass spectrometry	MS
Murashige Skoog	MS
Nicotinamide adenine dinucleotide phosphate	NADP+
N-terminal acetyltransferase	NAT
N-terminal acetylation	NTA
Oxygen-evolving complex	OEC
Polyacrylamide gel electrophoresis	PAGE
Post-translational modifications	PTMs
Photosystem	PS
Plastoquinone	PQ
Reduced nicotinamide adenine dinucleotide phosphate	NADPH
Rubulose biphosphate carboxylase oxygenase	Rubisco
Rubisco activase	RCA
Rubisco large subunit	RBCL
Rehydration Buffer	RB
Sodium dodecyl sulfate	SDS
Solubilization buffer	SB
Wild-type	WT

1. Introduction

1.1 Protein acetylation

Protein acetylation describes catalytic or non-catalytic transfer of an acetyl group from an acetyl-containing compound (most often Acetyl-CoA) to the protein (Lehtimäki et al. 2015). The free amino groups are the target of the acetyl transfer. Hence, Acetyl-CoA (Ac-CoA) is the major substrate for protein acetylation (Drazic et al. 2016). Ac-CoA is generated by multiple pathways in the cell, including glycolysis (from pyruvate) and β -oxidation of fatty acids. It can also be generated from citrate by Ac-CoA-citrate lyase (ACL), and acetate by Ac-CoA synthetase (AceCS) (Drazic et al. 2016). The mitochondria contain pyruvate dehydrogenase, citric acid cycle components, and an enzyme apparatus for β -oxidation. There are two distinct isoforms of AceCS - AceCS1 and AceCS2. They are located in the cytoplasm and the mitochondria, respectively.

For most of its history, acetylation research focused on eukaryotes regarding chromatin maintenance and gene expression. But it changed in the late nineties. Recent studies indicate that bacterial protein acetylation has significance in virulence, transcription, translation and also regulating central and secondary metabolism (Drazic et al. 2016). Three kinds of protein acetylation have been identified so far: N-terminal acetylation (NTA), lysine (Lys, K) acetylation (Lys acetylation) and O-acetylation. O-acetylation, which occurs at the hydroxyl group of Ser or Thr residues, has been found only in bacterium *Yersinia pestis* (Mukherjee et al. 2006). Whereas N-terminal and Lys acetylations have been reported to occur in all kinds of organisms; and as their names suggest they occur in N-terminal amino acid and internal Lysine side chain, respectively (Lehtimäki et al. 2015).

Protein acetylation is primarily catalyzed by acetyltransferase enzymes. Both N-terminal and lysine acetylation follow the same basic mechanism - the transfer of an acetyl group from acetyl-coenzyme A. In case of NTA, the transfer happens to the α -amino group of the protein N-terminal amino acid, and in case of Lys acetylation, to the ϵ -amino group of lysines. Despite the basic similarity, these two acetylations have their dissimilarities too. Lys acetylation is a post-translational and reversible modification. On the other hand, NTA is co-translational and irreversible (Drazic et al. 2016) (Figure 1). In some exceptional cases, NTA can happen post-translationally, too (Allis et al. 2007).

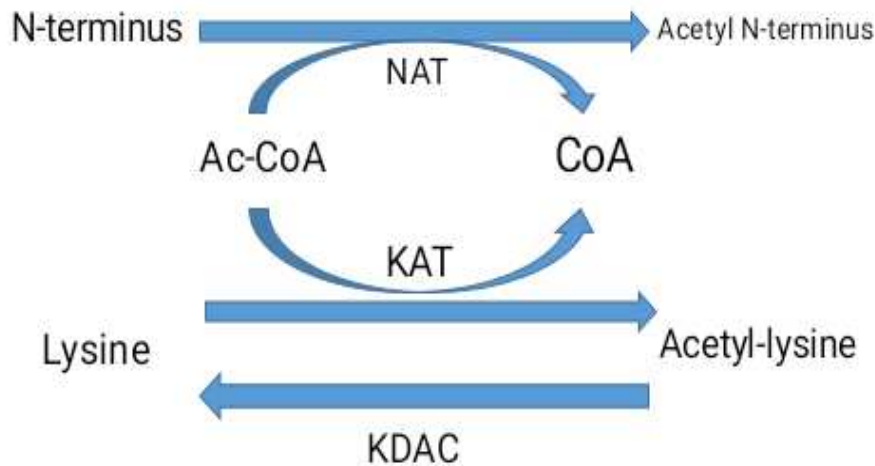


Figure 1: Schematic diagram of N-terminal and lysine protein acetylation. N-terminal acetyltransferases (NATs) and Lysine acetyltransferases (KATs) catalyze the transfer of an acetyl group from Ac-CoA to the free α -amino group of protein N-termini and to the ϵ -amino group of lysine side chains, respectively. NTA is considered irreversible because an N-terminal deacetyltransferase (NDAC) is not discovered yet. In the case of lysine acetylation, it is considered a reversible protein modification as the acetyl moiety can be removed by Lysine deacetylase (KDACs).

It has been observed that the propensity of these modifications increases with organism complexity (Drazic et al. 2016). In multicellular organisms, Lys acetylation occurs in all the major cell organelles, nucleus and cytoplasm, whereas NTA mostly occurs in cytoplasmic proteins (Varland et al. 2015). Regardless of these facts, previous studies have indicated that both of these modification types are prevalent in chloroplasts - which host both plastid and nucleus encoded proteins (Pozoga et al. 2022).

The enzymes that catalyze lysine (K) acetylation were initially named histone acetyltransferases (HATs) because lysine acetylation was first found in histones controlling gene transcription (Allfrey et al. 1964). However, lysine acetylation is not restricted to histone proteins. And that's why, later the enzymes have been renamed as KATs (Allis et al. 2007). While the recognized KATs are categorized in at least three families (Gcn5/PCAF, MYST, and p300/CBP), all the N-terminal acetyltransferases (NATs) which have been discovered so far are members of the superfamily of general control non-repressible 5 (GCN5)-related N-acetyltransferases (GNATs) (Friedmann and Marmorstein, 2013; Drazic et al, 2016). It is known that several families of KDACs are involved in counteracting KATs. In many cellular processes, KATs and KDACs establish a complex and balanced interplay in the regulatory network (Drazic et al. 2016).

1.1.1 N-terminal acetylation

NTA is irreversible and prevalent in eukaryotes, including plants. The function of the modification is to neutralize the N terminus positive charge, resulting in isoelectric point (pI) shift of the protein - making it more acidic. A family of NATs catalyzes NTA both in the

cytoplasm and chloroplast (Arnesen et al. 2011; Linster et al. 2018). These complexes are often ribosomes-associated. NATs transfer an acetyl group from Ac-CoA to a newly synthesized polypeptide chain's positively charged free α -amino group (Arnesen et al. 2011; Linster et al. 2018). This positive charge is neutralized by the linked acetyl group, which also often prevents further modification of the N-terminus (Arnesen et al. 2011; Linster et al. 2018). The reaction happens after initiation Methionine residue (iMet) is removed by ribosomal-bound methionine aminopeptidases (MetAPs), or the acetyl group is transferred to the non-cleaved iMet of the polypeptide chain, depending on the NAT (Arnesen et al. 2011; Linster et al. 2018). Not every possible NAT substrate has all of its N-termini acetylated. Since partial NTA is frequent, a protein may coexist in the cell in both its acetylated and unacetylated forms (Arnesen et al. 2011; Linster et al. 2018). Structural studies have provided information about the catalytic mechanism of NATs in recent years (Bienvenuet et al. 2020).

NATs can be either mono- or multisubunit. They have a catalytic subunit as well as one or more auxiliary subunits. The catalytic subunit's activity and substrate specificity are regulated by the major auxiliary subunit (Liszcak et al. 2013). The first two amino acid residues often dictate the substrate specificity of each NAT (Starheim et al. 2012). NatA acetylates the N-termini of Serine, Alanine, Threonine, Valine, Glycine, and Cysteine. This reaction occurs in proteins which have their iMet removed (Polevoda et al. 1999). Proteins which have their iMet intact and an acidic or hydrophilic amino acid residue are acetylated by NatB (Polevoda et al. 1999).

This modification is speculated to impact different molecular mechanisms and events in different organisms such as protein targeting (Behnia et al. 2004), determination of protein half-life (Bienvenuet et al. 2011), and mediation of protein-protein interactions (Scott et al. 2011) etc. A protein that in its N-terminally acetylated state exhibits different and consequential properties. For certain proteins, the subcellular localization is determined by NTA (Behnia et al. 2004). According to a different study, NTA suppresses a post-translational translocation movement to the endoplasmic reticulum and the secretory route (Forte et al. 2011). At the same time, the modification also restrains proteins in the cytoplasm. Protein-protein interactions appear to be regulated as a result of acetylation changes to the N-terminus (Forte et al. 2011). A recent article indicated NTA's role in protein folding (Scott et al. 2011).

In chloroplast proteins, three different kinds of NTA have been found. First one is the co-translational cytoplasmic acetylation of nuclear-encoded transit peptides. NatB and NatC are two examples of this kind (Van Damme et al. 2011). The second kind of NTA takes place inside the chloroplast following transit peptide excision. It involves post translational acetylation of nuclear-encoded proteins. Two examples of it are Ferredoxin-NADP Oxidoreductase (FNR) and Pyruvate Orthophosphate Dikinase (Lehtimäki et al. 2014). Third kind of acetylation involves either co- or post-translational NTA in the chloroplast and it targets chloroplast genome encoded proteins. Some of the examples are PSII core polypeptides D1, D2, the PSII CP43 reaction center protein, rubisco Large subunit (RBCL), and Adenosine triphosphate (ATP) Synthetase ϵ subunit (Hoshiyasu et al. 2013; Zybailov et al. 2008).

Despite the limitation of knowledge available, a recent study indicates a role for NTA in abiotic stress like drought. In the presence of the stress, the N-acetylated form of the APTE protein is more resistant against degradation by metalloaminopeptidases as compared to the nonacetylated APTE counterpart (Hoshiyasu et al. 2013). It proves the hypothesis that NTA plays certain roles in mediating environmental stresses in higher plants (Linster et al. 2015). Some other studies involving mutated strains of plants also point towards the physiological impact of NATs. Plants missing the homolog of NatC demonstrated aberrant structure and disruption of photosynthesis (Pesaresi et al. 2003). Another study conducted in *Arabidopsis thaliana*, which lacked the cytoplasmic NatB complex, showed abnormalities in gametogenesis, fertilization, leaf development and flowering time (Huber et al. 2019).

1.1.2 Lys acetylation

Although historically known for its significance in transcriptional control through chromatin (histone) remodeling, recent studies have found numerous other Lys acetylated proteins. Two of them are encoded by the chloroplast genome (RBCL and ATP Synthetase β Subunit) (Lehtimäki et al. 2015). It was originally suggested that non-enzymatic autoacetylation is partly responsible for organellar Lys acetylation, as no presence of Lys acetyltransferase or deacetylase was found at the time (Lehtimäki et al. 2015). In both of the above-mentioned proteins, Lys acetylation is found in either the catalytic center of the enzymes or in its proximity.

Gcn5/PCAF, MYST, and p300/CBP are the three superfamilies known to contain KAT (Allis et al. 2005). Gcn5/PCAF family consists of Gcn5, PCAF and other related proteins. They constitute one of the major groups of nuclear HATs. According to many studies, these HATs function as transcriptional coactivators that acetylate histones. PCAFs are found to acetylate histones as well as non-histone proteins (Koutelou et al. 2021). Another major group of nuclear HATs is p300/CBP. They are also transcriptional co-activators. Both p300 and CBP are capable of acetylating both histone and non-histone proteins. In *Arabidopsis thaliana*, five novel proteins with sequence similarity to HATs domain were discovered (Longo et al. 2022). A third major group of nuclear HATS are hosted in the MYST family. This family is more diverse, larger but relatively less explored and attributed compared to the other two major families mentioned. Although different MYST family proteins have similarities in their HATs domains, when it comes to functionality, they are quite varied in their roles (Utley and Côté, 2003).

The enzymatic counterpart of KATs - a class of deacetylase KDACs named the sirtuins, use nicotinic adenine dinucleotide (NAD⁺) as a co-substrate (Choudhary et al. 2009). These two metabolites connect cell signaling pathways and cellular metabolism, making them significant hubs of cellular metabolism. Since lysine acetylation may be reversed, unlike NTA, it is an essential mechanism for the cell for the activation and deactivation of specific pathways. In addition to lysine acetylation catalyzed by KAT, acetylation processes can also happen non-enzymatically through direct protein-Ac-CoA interaction. Many cellular functions, including chromatin-based transcriptional regulation, depend on the balanced regulation of KATs and KDACs (Peserico and Simone, 2011).

There are other known substrates of KAT complexes besides histone proteins. KATs regulate a wide variety of transcription factors and co-factors (Yang, 2004). Thus, KATs are essential

regulators of transcriptional and epigenetic control. In addition to nuclear substrates, cytosolic proteins are included in the large pool of substrates that KATs can bind to. KAT autoacetylation is widespread and appears to have varied functions for various KATs. Histone and non-histone proteins can be acetylated individually or in the PCAF complex by the HATs named p300 and CBP. This process can result in autoacetylation at different lysine residues (Thompson et al. 2004). Autoacetylation raises KAT activity in both situations. The catalytic region of both enzymes includes lysine residues, where autoacetylation occurs. Subsequent acetylation and substrate binding require these acetylation reactions first (Yuan et al. 2011).

Histones were the first proteins to be found to be acetylated (Allfrey et al. 1964). Different groups of HATs acetylate the histone core proteins - H2A, H2B, H3, and H4. Histone proteins combine with DNA to produce what are known as nucleosomes. Nucleosome chains' interactions lead to the formation of distinct chromatin structures, These structures may or may not be transcriptionally active. Numerous post-translational modifications (PTMs) modify the histone molecules. Among them, methylation, phosphorylation, and acetylation are deemed to be the most important for DNA accessibility and transcriptional control. Histone acetylation controls the transformation between transcriptionally active and inactive chromatin structure. The modification does it by regulating how histones assemble, fold and the compactness of histone-DNA interaction (Eberharter and Becker, 2002). The histone proteins undergo temporary acetylation following synthesis. The modifications dictate where the proteins are deposited and located inside the nucleus (Smith and Stillman, 1991).

Higher levels of acetylation are generally correlated with higher transcriptional activity. When an acetylated lysine side chain loses its positive charge, the side chains' capability of forming salt bridges with the phosphate backbone of DNA histone decreases substantially. Thus, acetylation results in the destabilization of DNA-histone interaction. This culminates in an open, loosely packed chromatin structure known as euchromatin, which propagates gene transcription. The opposite structural state - heterochromatin describes the tight packaging of chromatin. It has been shown that fiber production and dense chromatin structure are especially dependent on residues 14–23 of histone 4's tail. When these residues are acetylated, particularly H4K16, the chromatin structure is perturbed. As a result, transcription is activated and the euchromatin form is preserved. Histone-DNA interaction is disrupted by the acetylated H3K64, H3K56, and H3K122 (Peterson and Laniel, 2004). H4K91 acetylation affects H2A-H2B dimer formation - causing structural change in chromatin and weakening of the histone octamer. (Ye et al. 2005).

In plants, Lys acetylation is speculated to affect enzyme activity and enzyme-substrate interactions. Ribulose bisphosphate carboxylase oxygenase (Rubisco) enzyme activity is greatly impacted by this modification. The small subunit of rubisco and rubisco activase are the primary targets of it. Moreover, a study showed an increase in Rubisco catalytic activity as a consequence of in vitro deacetylation of RBCL derived from *Arabidopsis* (Gao et al. 2016). Furthermore, Lys acetylation has been suggested in the regulatory process of LHCB1 and LHCB2 association with PSII (Lehtimäki et al. 2015).

1.2 Chloroplast acetyltransferases

The enzymes that catalyze acetylation reactions in chloroplast belong to the GNAT superfamily (Bienvenut et al. 2020; Ivanauskaite et al. 2023). Ten putative chloroplast GNATs (GNAT1–10) have been identified so far (Bienvenut et al. 2020). Seven of them had their chloroplast localization verified by an extensive study (Bienvenut et al. 2020). These GNATs have some differences in the N- and C-terminal regions, but they share conserved structural domains involved in substrate binding and acetylation (Bienvenut et al. 2020). Although the sequence homology among the organisms are relatively low, the GNATs enzymes found in them share common secondary and tertiary structures (Bienvenut et al. 2020).

All of the ten putative GNATs proteins discovered so far in *Arabidopsis* plastids have shown both NTA and KTA activities (Bienvenut et al. 2020). Their catalytic activity on the basis of amino acid sequence could not be inferred. So, these proteins were given the designation GNAT1–10 (Bienvenut et al. 2020). A phylogenetic distance tree with recognized GNAT proteins to understand the evolutionary relationship. According to their findings, *Arabidopsis* GNAT1-3 formed the first subtype of GNAT-related sequences. GNAT4-7, and 10 belong to a distinct branch whereas GNAT8 and GNAT9 were designated into a third subtype (Bienvenut et al. 2020). In the same study, the expected plastid locations were verified. It was done by constructing an expression system in *Arabidopsis* which expressed GNAT fusion protein with a C-terminal Green fluorescent protein (GFP) tag. The expression was carried out under the 35S promoter in *Arabidopsis* protoplast. The locations of GNAT1, 2, 3, 4, 5, 7, and 10 in plastids were verified by an overlap between GFP and chlorophyll autofluorescence. A spotted fluorescence pattern was seen in the GNAT6-GFP, which was determined to be either confined within the nuclear membrane or connected with chloroplasts. The GNAT6-GFP fluorescence did not overlap with mitochondria, according to mitotracker labeling. Protoplasts harboring GNAT8 and 9 GFP displayed fluorescent signals similar to free GFP which points to cytosolic/nuclear location (Bienvenut et al. 2020).

Apart from the anticipated transit peptide, every chloroplast GNAT possesses the conserved GNAT structure, which is composed of four α -helices and six β -sheets that constitute domains A–D. According to a study, domain A has the active site; whereas domain B is essential for substrate binding. Domains C and D are proposed to have potential impact on protein stability. The most diverse regions are located in the N- and C-terminal. These regions influence substrate specificity and binding to putative auxiliary proteins. A secondary substrate binding site were found in GNAT1-4, GNAT7, and GNAT10 (Bienvenut et al. 2020).

The same study conducted a global Lys-acetylome analysis in order to thoroughly define the activities of all chloroplast GNATs. Using a T7 promoter in *E. coli*, eight GNAT proteins were expressed. Those proteins lacked their predicted target sequence. They also expressed an N-terminal His-tag and a maltose-binding protein in the same construct. All proteins exhibited a noticeable overexpression following IPTG-induced transcription. Upon extraction, they used a primary anti-acetyl lysine antibody to identify proteins which presumably are acetylated. The goal of the identification was to determine the functional possibility of the recombinant proteins as KAT enzymes (Bienvenut et al. 2020). The

Western blot analysis revealed a distinct pattern of Lys acetylation on *E. coli* proteins under non-induced circumstances. Nearly all GNAT recombinant proteins showed Lys hyperacetylation upon GNAT expression activation (Bienvenut et al. 2020).

The potential NTA activity and substrate specificity of this GNAT family had been examined in order to complete their characterisation. The Global Acetylation Profiling (GAP) assay, which exploits the recombinant expression of GNATs in the host organism *E. coli*, was used for this work (Dinh et al. 2015). The in cellulo technique, which is comparable to the Lys-acetylome profiling study, offers the NTA characterisation of the protein N-termini. The technique itself is only dependent on the biosynthesized protein. For the eight GNATs, the GAP assay identified around 397 protein N-termini. The *E. Coli* proteome showed a substantial increase in the quantity of N-terminally acetylated substrates upon treatment with six of the eight GNATs. GNAT1 and GNAT3 showed low substrate retrieval rate and also low efficiency for protein N-terminal and Lys acetylation, as the few substrates of GNAT3 were only slightly N-acetylated. It is likely that these two GNATs function exclusively on a limited range of distinct plastid substrates that are not present in the proteome of *E. coli*, or they need accessory proteins exclusive to plants, such as cytosolic N-terminal acetylases, to enhance their activity. On the other hand, the maximum number of acetylated N-termini were generated by GNAT 4, 6, and 7. GNAT10 provided the lowest numbers and the lowest NTA yield increase. GNAT2, 5, and 10 produced the second most yield. However, the NTA and Lys acetylation activity are found to be unaffected by the biosynthesis of each GNAT. These chloroplast enzymes showed relatively relaxed substrate specificity, unlike cytosolic NATs. But they vary in their substrate preferences. The six most enzymatically efficient chloroplast GNATs were all very efficient for N-termini starting with an initiator methionine. But the second amino acid brought different substrate preference for them. GNAT10 acted mainly like NatC/E/F when it came to substrate preference. On the other hand, GNAT2, 4, 5, and 7 showed similar preference to NatA (Bienvenut et al. 2020).

Chloroplast acetyltransferases might have significance in modulating metabolic activities which play important roles in plant physiology. Studies show that GNAT2 affects thylakoid dynamics significantly and is crucial for state transitions (Koskela et al. 2018, Rantala et al. 2022). GNAT1 and GNAT2 are also involved in the production of melatonin and show dual enzymatic activity (NTA and KTA) (Bienvenut et al. 2020; Lee et al. 2014). In *Arabidopsis*, both GNAT1 and GNAT2 acetylate precursor serotonin and 5-methoxytryptamine (5-MT) in order to synthesize melatonin. But as mentioned earlier, they show preferences. While GNAT2 is more effective in 5-MT acetylation, GNAT1 prefers serotonin as a substrate (Lee et al. 2014).

1.3 GNAT2 and its effect on physiology

Among all the discovered GNATs, GNAT2 was the first enzyme which was attributed to have a regulatory role in the photosynthetic light reactions. As mentioned earlier, GNAT2 is responsible for state transitions and melatonin synthesis. But it doesn't simply end there. It plays a crucial role in other physiological activities as the studies involving GNAT2 mutation shows.

WT plants increase their melatonin levels in response to stresses such as avirulent diseases or strong light, while *gnat2* mutant plants do not (Lee et al. 2014, Leverne et al. 2023). Stress

tolerance may be connected to GNAT2-dependent melatonin generation, as seen by the *gnat2* mutants' decreased melatonin accumulation and greater vulnerability to stress. The plastid GNATs' impact on the biosynthesis of melatonin was also investigated (Ivanauskaite et al. 2023). But neither melatonin nor any of the intermediates in the melatonin biosynthesis pathway were found using the untargeted metabolomic technique. However, they employed a different UPLC-MS method (in accordance with Lee and Back, 2018) to find melatonin in the *gnat2* mutants. They found out that melatonin levels in the *gnat2* mutants were marginally elevated rather than decreasing. These findings suggest that, in ordinary growth conditions, GNAT2 is not required for the synthesis of melatonin (Ivanauskaite et al. 2023).

The importance of GNAT2 with respect to state transition was also explored (Koskela et al. 2018). When light conditions vary, PSI and PSII dynamically redistribute excitation energy. This process is called state transitions in photosynthesis. In chloroplasts, this process aids in maximizing light absorption and energy conversion. The LHCII proteins undergo reversible phosphorylation during state changes. Protein phosphatases and kinases control this phosphorylation. Phosphate-adding enzymes are known as kinases. LHCII is phosphorylated by a kinase under low light, which facilitates its association with PSI and amplifies its absorption of light. Enzymes called phosphatases work to eliminate phosphate groups. Phosphatases dephosphorylate LHCII in high light, facilitating its association with PSII for the optimal light harvesting. The thylakoid membrane protein kinase STN7 phosphorylates LHCII in low light, while STN8 phosphorylates PSII core proteins in high light.

Blue native gel electrophoresis analysis revealed that thylakoid protein complexes derived from *gnat2* mutants did not include the PSI-LHCII supercomplex (Koskela et al. 2018). This supercomplex is responsible for state transition that is usually detected in low to moderate light (Kouřil et al. 2005). As growth and red light conditions induce the formation of the PSI-LHCII supercomplex, measurement of the 77K fluorescence emission spectra of thylakoids extracted from plants grown in those conditions revealed that the fluorescence emission peak of PSI (735 nm) was significantly lower in the *gnat2* mutant (Koskela et al. 2018). On the other hand, the same measurement didn't result in any difference when it came to thylakoid samples extracted from plants grown in dark and far-red light conditions - which are known to induce PSI-LHCII supercomplex dissociation (Koskela et al. 2018). Those studies concluded that, in the *gnat2* mutant, the phosphorylated LHCII trimer cannot bind to the PSI complex. This is the reason why the LHCII timer cannot redistribute excitation energy to PSI.

According to the studies, rearrangements of the thylakoid protein complex and state transitions depend on the phosphorylation of LHCII (Kyle et al. 1983; Pietrzykowska et al. 2014). According to an immunoblot analysis done as part of a recent study (Koskela et al. 2018), it was revealed that *gnat2* mutants exhibit enhanced phosphorylation of LHCII proteins. Moreover, transmission electron microscopy showed that, compared to the wild type, *gnat2* mutants' grana stacks were found to be more densely packed (Koskela et al. 2018). Circular dichroism (CD) spectroscopy revealed alterations in the LHCII composition and complex stability in *gnat2* mutants. Unlike the wild type, light-induced thylakoid dynamics were negligible in *gnat2*, suggesting that LHCII mostly remained in the appressed fraction in the mutant (Rantala et al. 2022).

According to the another study (Ivanauskaite et al. 2023), under specific light conditions, *gnat2* mutants displayed a slight growth retardation. Also, in *gnat2* mutants, the ratio of chlorophyll a to b was marginally reduced. Furthermore, *gnat2* mutants showed increased nonregulated energy dissipation and decreased PSII yield. In light intensities above growth light, non-photochemical quenching (NPQ) was increased in *gnat2* mutants, as did the LHCI protein phosphorylation. Also, all *gnat* mutants exhibited increased Rubisco and RCA accumulation. However, in studied *gnat1*, *gnat2* and *gnat10* mutants, the increased Rubisco and RCA had no effect on CO₂ assimilation.

The change in state transition in *gnat2* mutants may contribute to higher drought resistance (Leverne et al. 2023). In order to examine the mutants' tolerance to drought, the wild type, *nsi1* (*gnat 1* homolog), *nsi2* (*gnat 2* homolog), and *stn7* were deprived of water for a period of six days. The state transition mutants' leaves showed clearly less effects than the wild type leaves, which withered. In plants that received adequate water, the rosette diameters of the various genotypes were comparable. In order to create a moderate drought stress, water was withheld for four days during the subsequent trials. Photosynthetic electron transport is not thought to be the main source of harm in this scenario. When the mutants were subjected to mild drought stress, their rosettes displayed significantly more water content. During severe drought stress, wild type plants showed relative stomatal closure, whereas mutants did not. The study also looked into how moderate drought affects photosynthesis since the mutants' capacity to adjust their antenna size based on stress conditions, light quality, and intensity. Between the genotypes under drought stress and those without, there were no significant differences in the compositions of carotenoid and chlorophyll. All genotypes showed an increase in β -carotene, lutein, and neoxanthin content upon the drought. Chlorophyll fluorescence parameter analysis revealed that while there were no appreciable changes in the mutants, the drought had a considerable impact on the wild type PSII's effective quantum yield. The seedlings' root growth was also examined. In comparison to the mutants, the wild type's main root was shorter and thinner. Furthermore, in the mutants, lateral development of roots was markedly increased. Four-week old soil grown plants also displayed differences in root development. The wild type showed a significantly less developed root system.

1.4 Photosynthesis

Photosynthesis is a set of complex anabolic reactions that is present in many prokaryotic and eukaryotic forms of life. Solar energy harvesting, excitation energy transfer, energy conversion, electron transfer from water to NADP⁺, ATP synthesis, and a sequence of enzyme processes that assimilate carbon dioxide and manufacture carbohydrates are all included in this process.

The process of photosynthesis initiates with light reactions. Absorption of light by the pigments occurs in the first step. Different forms of chlorophylls are the primary component of these pigments. Tetrapyrrole rings and magnesium are the basis of chlorophyll pigment. Additionally, a long side chain is attached to each ring. Two forms of chlorophyll, called a and b, expand the range of wavelengths absorbed in plants.

1.4.1 Photosystems and LHC complexes

Two photosystems, PSI and PSII, are crucial part of the chloroplasts' photosynthetic apparatus and has a complicated structure designed to facilitate effective light absorption and

electron transfer during photosynthesis. Within the thylakoid membrane, PSII is made up of a reaction center called P680, which is used to transform light energy into chemical energy. Antenna pigments, such as molecules of chlorophyll, are present to absorb photons. The oxygen-evolving complex (OEC), which is essential for water splitting, is also included in PSII. On the other hand, PSI, which is situated within the thylakoid membrane as well, has an antenna pigment connected with a reaction center called P700. PSI receives electrons from PSII and performs downstream tasks in the electron transport chain. In plants, two complexes - LHCI and LHCII are responsible for absorbing light. These complexes consist of chlorophyll a, b, and carotenoid pigments. LHCI and LHCII are composed of Lhc proteins and serve as antennas for PSI and PSII. LHCI complex consists of Lhca1-4 proteins whereas LHCII consists of Lhcb1-3 proteins. In *Arabidopsis*, minor PSII antenna proteins Lhcb4-6 (CP29, CP26, and CP24) link LHCII to PSII. Both PSII and PSI receive excitation energy from LHCII heterotrimers (Kok 1959; Döring et al. 1969).

1.4.2 Photosynthetic electron transfer

In a process called photosynthetic electron transfer, both PSs work together to gather light energy and transform it into chemical energy through a sequence of redox processes. This process ultimately makes it easier for the plant to synthesize ATP and reduced nicotinamide adenine dinucleotide phosphate (NADPH). In this process, PQ is a key molecule in the electron transport chain that is actively involved in the production of ATP. PSII is responsible for transferring light energy to it. Through a process called photolysis, the oxidized reaction center pigment P680 recovers its reduced state by removing electrons from water, producing oxygen as a byproduct. PSI can also absorb light energy. The protein ferredoxin receives electrons from its reaction center pigment P700. Ferredoxin can then donate the electrons to the electron carrier NADP⁺ to make NADPH or to the electron transport chain to produce more ATP.

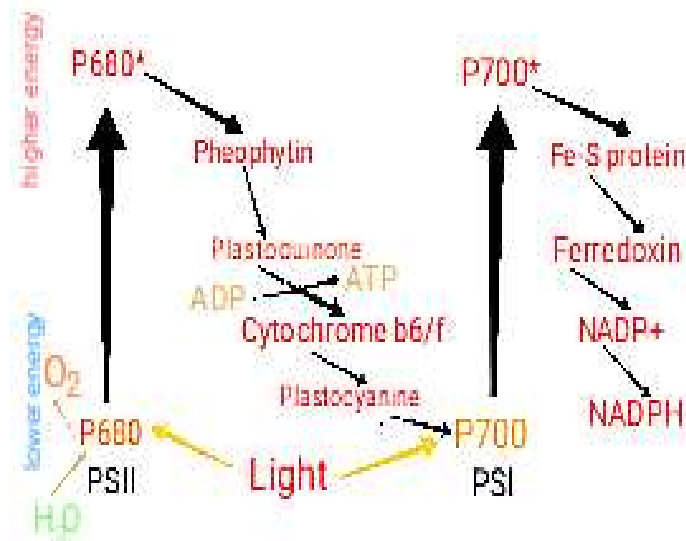


Figure 2: Diagrammatic representation of the photosynthetic electron transfer (the photosynthetic Z-scheme). It involves the redox reactions during the light phase of photosynthesis, in which electrons are removed from water (to the left) and then donated to the lower (non-excited) oxidized form of P680 as well as culminating in the synthesis of ATP and NADPH.

1.4.3 Carbon assimilation

Carbon assimilation takes place during the in the chloroplast stroma, in which the Calvin cycle utilizes the ATP and NADPH that the light-dependent reactions of the PSs produce. It consists of three major reactions which are carboxylation, reduction, and regeneration. The enzyme Ribulose biphosphate carboxylase oxygenase (Rubisco) catalyzes the first reaction of the cycle. In this reaction, a one-carbon molecule CO₂ reacts with the five-carbon compound ribulose biphosphate, or RuBP, forming an unstable product that disintegrates right away to produce two molecules of the three-carbon compound phosphoglyceric acid, or PGA. In the Reduction stage, PGA is subsequently reduced to phosphoglyceraldehyde (PGaldehyde) using the energy of ATP and the reducing power of NADPH. In order to regenerate molecules of the original five-carbon complex (RuBP) from molecules of the three-carbon component (PGaldehyde). ATP is also required in the regeneration step. On the other hand, some of PGaldehyde are subsequently transformed into glucose in the plant cell's cytoplasm.

1.4.4 PSII structure and biosynthesis

From a functional perspective, PSII is a water:PQ photo-oxidoreductase (EC number 1.10.3.9) that catalyzes the oxidation of water to molecular oxygen and protons and the light-driven reduction of PQ to plastoquinol. The PSII core complex, also known as the central region of PSII, is structurally conserved and consists of four large membrane-intrinsic subunits - namely PsbA, B, C, and D. The two central subunits PsbA (D1) and PsbD (D2) together form a pseudo-heterodimer. It also has 35 chlorophylls, 10 β-carotenes, and various other cofactors (Müh and Zouni 2020). The core complex of heterodimeric reaction center of the D1 and D2 subunits is attached to the chlorin cofactors that are involved in the first stages of light-induced charge separation that result in the reduction of PQ and the oxidation of water. The reaction center receives light energy that is absorbed by the inner antennae, CP47 and CP43, which are symmetrically attached to D2 and D1, respectively. This process drives charge separation. Moreover, CP43 and D1 work together to ligate the Mn₄CaO₅ metal cluster, which oxidizes water. Several smaller transmembrane subunits with fewer understood functions surround these larger subunits. Different sets of proteins bind to PSII's luminal side in order to maximize the Mn₄CaO₅ cluster's function, in contrast to the protein's highly conserved core. There is even much greater diversity among the peripheral light-harvesting complexes that interact with PSII to generate large PSII supercomplexes (Johnson and Pakrasi, 2022).

Assembly of PSII is a well-coordinated de novo procedure. PSII assembly in higher plants consists of the following: (1) assembly of the precursor D1-PsbI (pD1-PsbI) and D2-cytochrome b559 (D2-Cyt b559) precomplexes; (2) assembly of the minimal reaction-center complex (RC), which doesn't contain CP47 and CP43; (3) assembly of the reaction-center complex (RC47a), which is CP47-containing but CP43-deficient; (4) incorporation of LMM subunits, including PsbH, PsbM, PsbT, and PsbR, to form RC47b, The OEC-less PSII monomer is formed by the following steps: (5) CP43 inclusion; (6) OEC assembly; (7) dimerization and creation of the PSII-LHCII supercomplex; and (8) assembly of the OEC and extra LMM subunits, such as PsbW and PsbZ (Nickelsen and Rengstl, 2013).

1.5 Arabidopsis thaliana

Arabidopsis thaliana, commonly known as the Thale Cress, is a small dicotyledonous plant in the mustard family. Over the years, the plant has become the most common model organism for research in eukaryotic plant biology and its features carry the testament for the choice. This little plant grows well in laboratory settings, on shelves at room temperature and with little light. Its generation period is only about six weeks. Although cross-pollination is easily achievable, it generally reproduces via self-pollination. It produces between 10,000 and 30,000 seeds which is fairly large quantity. The seeds germinate to produce tiny seedlings that can be cultivated in petri dishes under regulated environmental conditions. Thus, while keeping other growth circumstances constant, it is possible to expose individual seedlings to varying quantities of a particular environmental parameters. Due to the capacity to cultivate a great number of *Arabidopsis* seedlings in extremely controlled environments, large-scale screens have been created to analyze a variety of mutant plants. Moreover, its tiny (125 Mb) nuclear genome has been fully sequenced and sequence archive is open source. In terms of transformation compatibility, *Agrobacterium tumefaciens* has the ability to transform the plants relatively readily, resulting in an enormous collection of T-DNA-insertion and transposon-mobilized lines. These lines can be utilized for both forward and reverse genetic approaches.

2. Aims of the study

So far, previous studies indicated the effect of the GNAT2 enzyme on thylakoid dynamics, state transitions, plant phenotype, acetylation level of chloroplast proteins as well as GNAT1's and GNAT2's involvement in the production of melatonin. As the detailed effects of GNAT enzymes on seed germination, root development, thylakoid protein acetylation and de novo synthesis of PSII are yet to be investigated, the aims of the study are:

1. To understand the effect of GNAT2 on thylakoid protein accumulation and acetylation of light-harvesting complex II (LHCII) proteins.
2. To assess the germination and root morphology of WT and *gnat2* knock-out mutant under standard conditions and osmotic stress.
3. To understand the role of GNAT2 and GNAT1 in the early stages of PSII biosynthesis in *Arabidopsis thaliana*.

3. Materials and Methods

3.1 Plant materials and growth conditions

For investigating the accumulation and distribution of chloroplast proteins in the *gnat2* mutant (SALK_033944), the *Arabidopsis thaliana* WT (Col-0) and *gnat2* knock-out mutants were grown using peat:vermiculite mixture (2:1) for five weeks under 12 h light/12 h dark cycles at a PPFD of $120 \mu\text{mol m}^{-2}\text{s}^{-1}$, +23 °C temperature and relative humidity of 50%. For investigating the impact of Lys-acetylation of the D2 protein on the PSII biosynthesis, WT (Col-0), *gnat1* (SALK_150736) and *gnat2* (SALK_033944) were grown for two weeks on nylon-web covered peat:vermiculite mixture (2:1) under the same conditions.

3.2 Root development and germination test

For root phenotyping and germination test, WT and *gnat2* seeds were sterilized using solution 1 (70% ethanol and 0.05% TritonX-100 buffer) for 2 minutes, solution 2 (70% ethanol) for 2 minutes and solution 3 (100% ethanol) for 1 minute, respectively. The seeds were plated on ½ strength MS (0.28% MS salt, 0.4% plant agar) vertical plates and grown under 16 h light/ 8 h dark cycles and +23°C temperature. To assess the same parameters under osmotic stress, the WT and *gnat2* mutant plants were also grown on ½ MS-plates with the stress induced by 200 mM mannitol. The schematic view of the workflow is presented in Figure 3.



Figure 3: The workflow for assessing the root genotype and seed germination in WT and *gnat2* mutants.

3.3 Isolation of thylakoids

About 7-8 rosettes were removed from *Arabidopsis* plants that were 5 weeks old. In case of 2 weeks old plants, the number were approximately around 50. These rosettes were then put in 80 ml of ice-cold P1 grinding buffer (330 mM sorbitol, 5 mM MgCl₂, 50 mM HEPES-KOH pH 7.5). 10 ml of NaF, 100 mg of BSA per 100 ml and 88 mg of ascorbate per 100 ml were added to the buffer right before the extraction. The leaves were put in the P1 buffer and thoroughly ground with seven 2-second pulses of an OBH nordica blender. After filtration through Miracloth, the resultant suspension was centrifuged at 5000 g for 5 minutes at 4°C in 50 ml Falcon tubes.

The pellet was resuspended in 15 ml of P2 shock buffer (5 mM MgCl₂, 50 mM HEPES-KOH pH 7.5) to disrupt chloroplasts. 10 mM NaF was added to the P2 buffer right before the extraction. It was followed by a second round of centrifugation. After centrifuging, 15 ml of P3 storage buffer (100 mM Sorbitol, 5 mM MgCl₂, 50 mM HEPES-KOH pH 7.5) was added to wash the remaining P2 buffer residue followed by the final round of centrifugation. Similar to the P2 buffer, 10 mM NaF was added to the P3 buffer before the extraction process. After carefully removing the supernatant, the pellet was resuspended in 100 μl of P3 buffer. After that, the samples were frozen in liquid nitrogen and stored at -80°C.

3.4 Chlorophyll concentration determination

The concentration of chlorophyll *a* and *b* and *a/b* ratio was determined according to Porra et al. 1989. Shortly, 1µl aliquot of the sample was suspended in 1 ml 20% acetone, 5% 12.5 mM Hepes-KOH pH 7.8 followed by vortex and centrifugation. Thereafter, A646.6 nm; A663.6 nm and A750.0 nm were measured by Berner UV-1800 UV spectrophotometer (Porra et al. 1989).

3.5 2D gel electrophoresis

The experiments involved running Isoelectric Focusing Electrophoresis (IEF) on the first dimension and 14% SDS-PAGE on the second dimension. The focusing was done using GE Healthcare's Ettan IPGphor 3. The pH range for the IEF covered was 3-8; and in order to get greater resolution, the range was covered in three overlapping pH windows (3-6 and 5-8). The workflow is shown in Figure 4.

3.5.1 IEF and SDS-PAGE

The BioRad 18-cm pH strips were used for IEF. The rehydration of the strips was done with 340 µl of Rehydration Buffer (RB) Working Solution per strip in an IPG box overnight. 100 Mm Dithiothreitol (DTT) and (0.2% w/v) IPG buffer were added to the RB stock (8 M urea, 2M Thiourea and 4% CHAPS) to formulate the RB Working Solution. The strips were placed gel side down on the solution. In a separate experiment, the thylakoid samples were treated with Solubilization Buffer (SB) (0.24% (w/v) Tris base, 48% (w/v) urea, 2% SDS) and DTT (0.62 % w/v) to enhance solubilization of light reaction center proteins.

For sample preparation, 100 µg of protein combined with RB Working Solution to a final volume of 150 µl before vortexing and centrifugation. The "eve_cup loading 18cm" protocol (75 µA/strip; no rehydration time; 20°C; 49250 total Vh; 150V step voltage for 3h, 300V step voltage for 3h, 1000V grad voltage for 6h, 10000V grad voltage for 2h, 10000V step voltage for 3h and 500V step voltage for 6h; in chronological order) was selected for IEF run. The focusing was run for 17 hours. The strips were denatured using EB+DTT and EB+IAA buffer solutions. These solutions were prepared by adding 30 mg DTT and 37.5 mg IAA separately to 1.5 ml EB buffer (375 mM Tris-HCl pH 8.8, 6 M Urea, 25% Glycerol, 2% SDS).

The second dimension SDS-PAGE gel was run at 14 mA (7 mA for each strip) overnight. After the run, the gels were stained with Coomassie R250 staining solution (0.1% Coomassie Blue R250 (w/w), 30% methanol, 5% acetic acid) for 1 hour and destained in a solution containing 30 % methanol and 5 % acetic acid for another hour. MQ water was used for storing the gels for a short period at 4°C. For longer preservation, 20% ethanol was used at the same temperature.

3.5.2 Gel imaging

Biorad GelDoc Go imaging system set to Coomassie Blue Gel White Trans was used for gel imaging. The selected exposure mode was Auto optimal and the image size was Large (width 21.0 × length 14.0).

3.5.3 Digestion and LC-ESI-MS/MS analysis

The potential spots showing significant pI shifts were cut from the 2D-gels and sent to the Turku Bioscience Proteomics lab for LC-ESI-MS/MS analysis. The proteins were digested in the proteomics lab using trypsin or chymotrypsin based on the predicted protein sequences.

According to the sample report provided by Turku Bioscience Proteomics lab, the LC-ESI-MS/MS analyses were performed on a nanoflow HPLC system (Easy-nLC1200, Thermo Fisher Scientific) coupled to the Q Exactive HF (Thermo Fisher Scientific, Bremen, Germany) equipped with a nano-ESI source. Peptides were first loaded on a trapping column and subsequently separated inline on a 15 cm C18 column (75 µm x 15 cm, ReproSil-Pur 3 µm 120 Å C18AQ, Dr. Maisch HPLC GmbH, Ammerbuch-Entringen, Germany). The mobile phase consisted of water with 0.1% formic acid (solvent A) and acetonitrile/water (80:20 (v/v)) with 0.1% formic acid (solvent B). A 30 min gradient was used to elute peptides (20 min from 6 % to 39 min solvent B and in 5 min from 39% to 100% of solvent B, followed by a 5 min wash stage with solvent B). MS data was acquired automatically by using Thermo Xcalibur 4.1 software (Thermo Fisher Scientific). A data dependent acquisition method consisted of repeated cycles of one MS1 scan covering a range of m/z 350 – 1750 followed by HCD fragment ion scans (MS2 scans) for the 10 most intense peptide ions from the MS1 scan.



Figure 4: The workflow for assessing the effect of GNAT2 on thylakoid protein accumulation and acetylation of LHCII proteins.

3.6 CN-PAGE

The experiment involved casting a gradient gel followed by sample preparation and running. In order to create a gradient, two solutions named of different concentrations were prepared which were aptly named light and heavy solutions. The differences in concentrations derived from the differences in volume of 75% (w/v) glycerol and acryl amide. The workflow is shown in Figure 5.

3.6.1 Gel preparation

A 3.5-10% gradient 0.75 mm large pore gel was used to resolve photosystem protein complexes. In order to develop the gradient, heavy (525 µl 40% acryl amide, 700 µl 3x gel buffer, 560 µl 75% glycerol, 295 µl MQ water, 11 µl 5% APS and 2 µl TEMED) and light (184 µl 40% acryl amide, 700 µl 3x gel buffer, 140 µl 75% glycerol, 1056 µl MQ water, 15 µl 5% APS and 3 µl TEMED) solutions were prepared and loaded into the Hoefer SG-5

loading chamber which was connected to ISMATEC IPC pump. The pump speed was set to 22 during acrylamide casting. Polymerization took around 1 hour.

3.6.2 Sample preparation, run and imaging

Thylakoid samples were diluted in 25BTH20G buffer [50 mM BisTris/HCl (pH 7.0), 40% (w/v) glycerol and 0.25 mg ml⁻¹ Pefa bloc, 200 mM NaF]. An equal volume of 2% beta-dodecylmaltoside (β -DM) (Sigma-Aldrich) in 25BTH20G buffer was added to the sample to achieve a final concentration of 0.5 mg ml⁻¹ of chloroplast and 1% β -DM in the sample and incubated on ice for 5 min. The membrane debris was pelleted by centrifugation at 18 000 g at 4°C for 20 min and the soluble protein complexes were used for the analysis. 1% Amphipol A8-35 detergent was used to give the complexes overall negative charges. The solubilized thylakoid protein complexes were separated with CN-PAGE (3,5–10% acrylamide). 10 μ g of Chl of each sample was loaded on the gel. Images of gel were captured using a digital scanner (Canon CanoScan LiDE 400), and fluorescent scan was done using LI-COR ODYSSEY CLx.

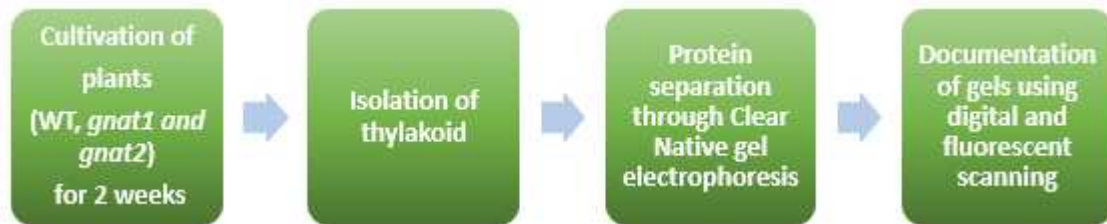


Figure 5: The workflow for assessing the role of GNAT1 and GNAT2 in the early stages of PSII biosynthesis.

3.7 Statistical analysis

T-test was conducted for both root length and seed germination data with Microsoft Excel software. The data derived from three for each biological replicate amassed in total sample numbers of 180 for plants grown under standard conditions and 90 for plants grown under osmotic stress. Obtained p-value under 0.05 was considered statistically significant.

3.8 Artificial Intelligence disclaimer

Quilbot AI was used to paraphrase some text used in different sections (Introduction, Materials and Methods, Discussion). The paraphrasing is followed by another round of paraphrasing by the author.

4. Results

4.1. Germination and root growth in WT and gnat2 plants

To find out how the loss of GNAT2 enzyme affects root development and seed germination, experiment was done with WT and *gnat2* mutant. Plants grown on ½ MS-plates (both optimal and osmotic stress conditions) showed decreased germination rate and retarded growth in *gnat2* mutant compared to its WT counterpart (Figure 6 and 7). The plants grown under standard conditions showed steady growth throughout the four weeks' period, whereas the plants grown under osmotic stress showed overall shorter growth and growth retardation after 2 weeks. These patterns were visible in both WT and *gnat2* plants. Three batches of plants were grown and each batch consisted of three plates per genotype (20 seeds/plate in standard conditions and 10 seeds/plate in osmotic stress). This resulted in a total sample size of 180 for each plant genotype under standard conditions and 90 for each plant genotype under osmotic stress conditions.

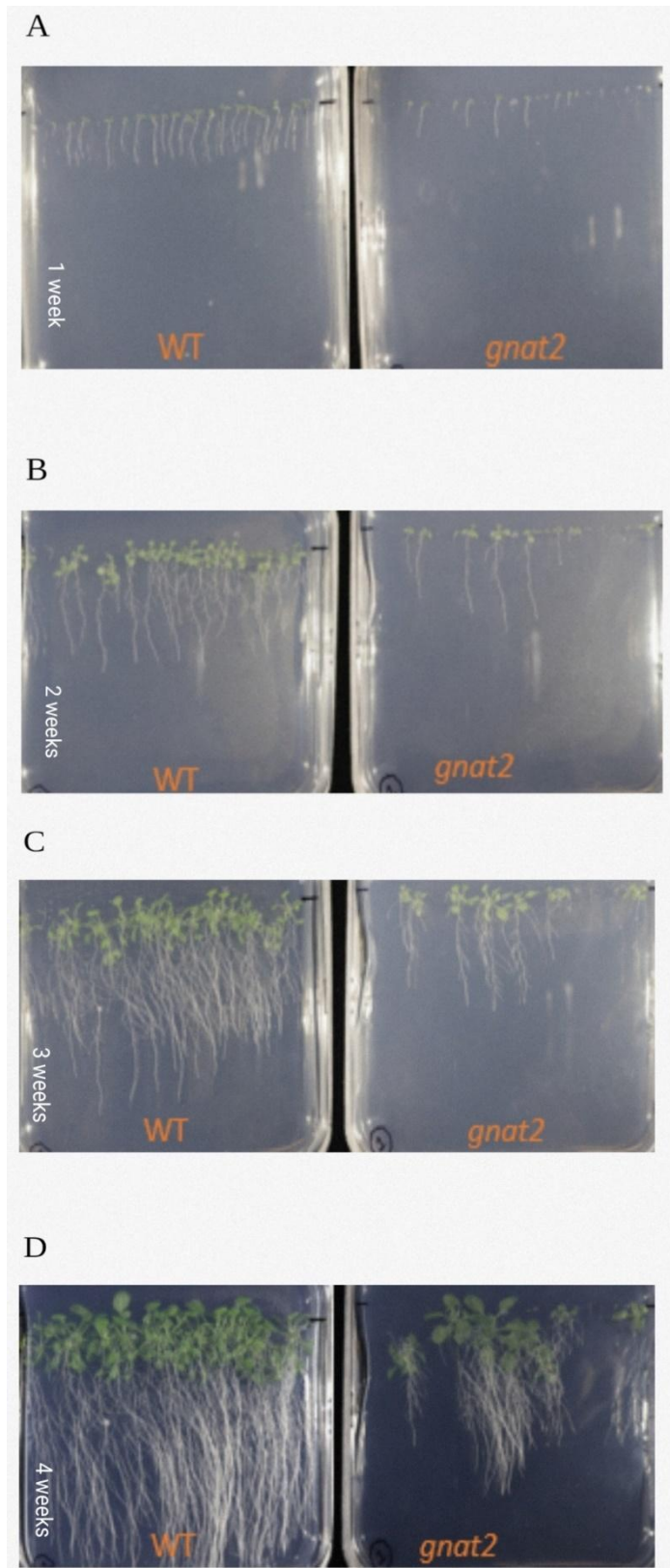


Figure 6: Root growth of WT and *gnat2* *Arabidopsis thaliana* plants grown on $\frac{1}{2}$ MS media under standard conditions for 1, 2, 3 and 4 weeks, respectively (Figure 6A, 6B, 6C and 6D).

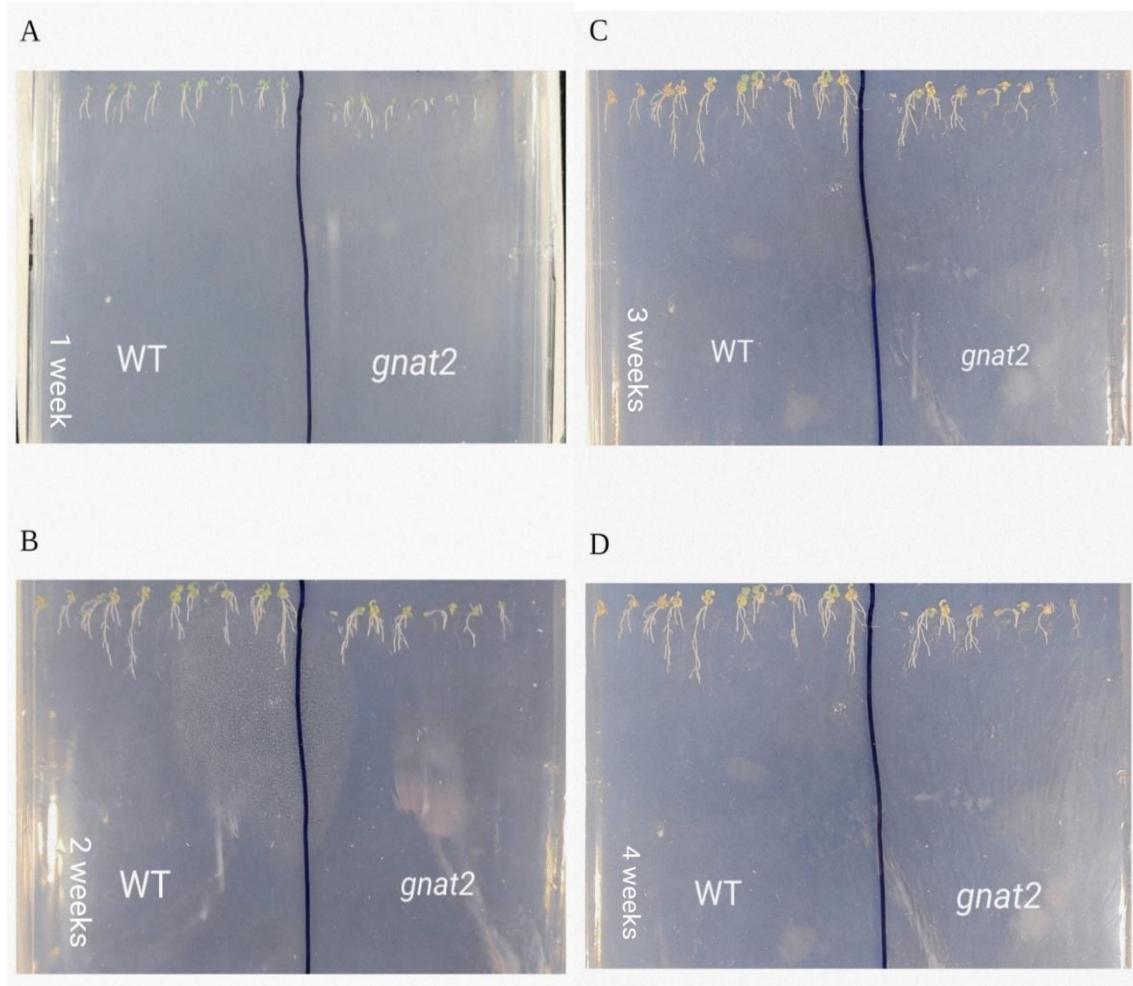
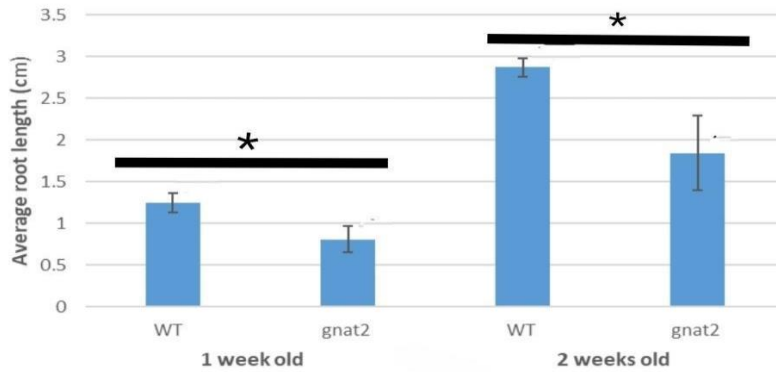


Figure 7: Root growth of WT and *gnat2* *Arabidopsis thaliana* plants grown on $\frac{1}{2}$ MS media under osmotic stress conditions for 1, 2, 3 and 4 weeks, respectively (Figure 7A, 7B, 7C and 7D).

There was a statistically significant decrease in root length for *gnat2* compared to WT under both standard and osmotic stress conditions (Figure 8A and 8B). Under standard conditions, 1 week WT plants showed a combined average root length of 1.2 ± 0.1 cm whereas the combined average root length for *gnat2* plants was 0.8 ± 0.1 cm. The growth pattern continued with a combined average root length of 2.8 ± 0.1 cm for 2 weeks old WT and 1.8 ± 0.4 cm for 2 weeks old *gnat2* plants. Also, under osmotic stress, WT plants showed a combined average root length of 0.5 ± 0.05 cm and 0.8 ± 0.1 cm for 1 and 2 weeks old plants, respectively, whereas the values were 0.29 ± 0.02 cm and 0.47 ± 0.01 cm for *gnat2* plants, respectively.

The t-test conducted with all the root length data points for 1 week and 2 weeks old plants grown under standard conditions resulted in p-values of 1.8×10^{-17} and 2.96×10^{-6} , respectively (Figure 8A), which confirms the statistical significance of the result datasets ($p < 0.05$). On the other hand, the same parameters for WT and *gnat2* grown under osmotic stress resulted in p-values of 1.3×10^{-9} and 6.7×10^{-4} , respectively (Figure 8B), which also confirms the statistical significance of the respective datasets ($p < 0.05$).

A



B

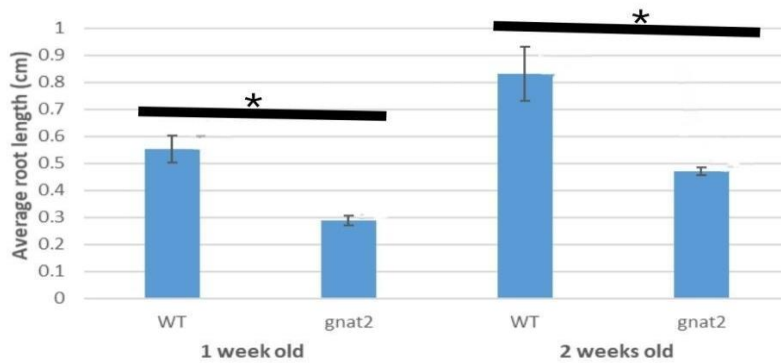


Figure 8: Combined average root length for WT and *gnat2 Arabidopsis thaliana* plants grown under standard and induced osmotic stress conditions. (A) Average root length in first two weeks under standard conditions. (B) Average root length in the first two weeks under osmotic stress induced by 200 mM mannitol. Error bars shown in the figures represent standard deviations and asterisks (*) represent the confirmation of statistical significance between the two dataset.

Plants grown under standard growth conditions showed an average germination rate of $98.3 \pm 1.6\%$ for WT whereas *gnat2* showed $71.7 \pm 4.7\%$ (Figure 9A). The t-test conducted resulted in a p-value of 1.045×10^{-8} (Figure 9A), which confirms the statistical significance of the result datasets ($p < 0.05$). Also, plants grown under osmotic stress showed an average germination rate of 100% for WT whereas *gnat2* showed $71.7 \pm 4.7\%$ (Figure 9B). The t-test conducted resulted in a p-value of 3.74×10^{-6} (Figure 9B) which confirms the statistical significance of the dataset ($p < 0.05$). So, there is a significant decrease in the combined average germination rate in *gnat2* compared to WT.

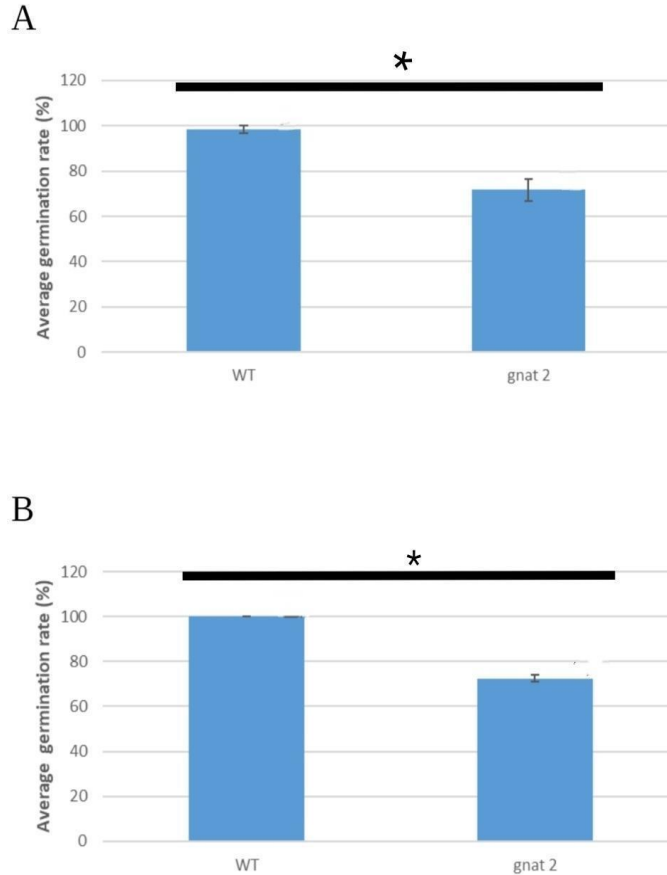


Figure 9: Average germination rate for WT and *gnat2* *Arabidopsis thaliana* plants grown under standard and induced osmotic stress conditions. (A) Average seed germination percentage under standard conditions. (B) Average seed germination percentage under osmotic stress induced by 200 mM mannitol. Error bars shown in the figures represent standard deviation.

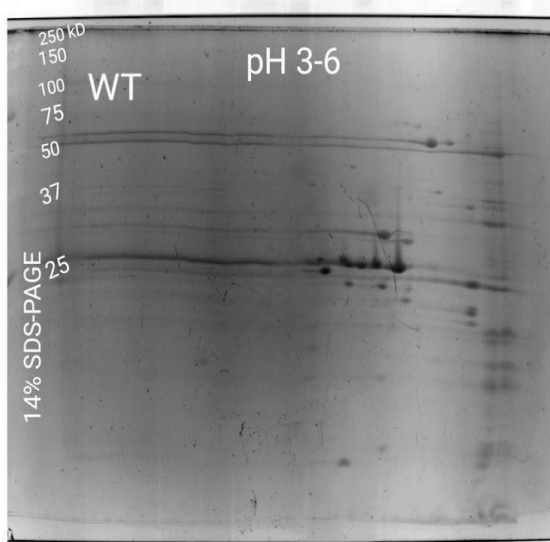
In the case of plants grown under standard conditions, from the third week on, root length measurement wasn't possible due to the entanglement of roots (Figure 6). Plates containing plants grown under osmotic stress also had fungal contamination problems after 2-3 weeks. They also showed stunted growth after 2-3 weeks even without contamination (Figure 7).

4.2. 2D gel electrophoresis of WT and *gnat2* thylakoid complexes followed by LC-ESI-MS/MS analysis

Loss of GNAT2 has been shown to affect the Lys and NTA level of several chloroplast proteins, but only a limited amount of acetylated thylakoid embedded proteins have been previously identified (Koskela et al. 2018, Bienvenut et al. 2020). Due to the limited coverage of proteome level acetylation data, some important acetylated proteins have remained undetected and uninvestigated. Therefore, plants were grown for 5 weeks followed by thylakoid isolation. The method chosen for protein separation was 2D gel electrophoresis with IEF in the first dimension and SDS-PAGE in the second dimension followed by Coomassie R250 staining. IEF-SDS-PAGE was chosen as a method of separation, because it enables the recognition of N-terminally acetylated proteins due to the associated shift in pI.

In the first attempt, 100 of μg proteins treated with RB working solution were separated by IEF strips in pH range 3-6 followed by 14% linear SDS-PAGE. In order to obtain high sensitivity for gel imaging, the gels were stained with SYPRO[®]. In both WT and mutant lines, approximately 15 spots were detected (Figure 10). However, Coomassie R250 staining was performed after that to ensure clear visualization for the purpose of cutting spots for MS analysis. The gel images showed changes in the pI of several protein spots when they were aligned vertically (Figure 11).

A



B

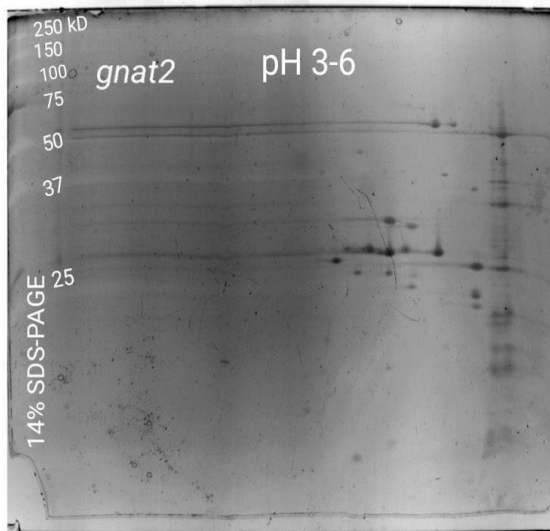


Figure 10: 2D-IEF-SDS-PAGE gel images of 100 μg of RB treated WT (A) and *gnat2* (B) thylakoid protein complexes in pH 3-6 ranges. SYPRO[®] was applied for staining.

When both gels were vertically aligned based on spots which didn't show shift in pI, six spots showed clear pI shift. These spots were chosen for LC-ESI-MS/MS analysis. These spots were designated as W1-W6 for WT and G1-G6 for *gnat2* (Figure 11), where each number indicates the supposedly same thylakoid proteins which show different pI in WT and *gnat2*. Spot number 2 was further divided into two (A and B) to separate partially overlapping spots. Based on the size and abundance of the protein spots, and previous analysis made by the group, it was hypothesized that the spots could represent LHCB-proteins. Hence, the digestion enzyme of preference was Chymotrypsin because it cleaves at the C-terminal of the amino acids phenylalanine, tryptophan, and tyrosine. As these residues are not located at the N-terminal of the expected LHCB proteins, the digestion results in MS compatible peptide fragments. Analysis of the spots revealed different patterns of acetylation - although common acetylations are shared between WT and *gnat2*, but there are unique acetylations for both WT and *gnat2* (Table 1). They also revealed that the NTA levels of LHCB1 and LHCB2 were decreased in the *gnat2* mutant (Table 2).

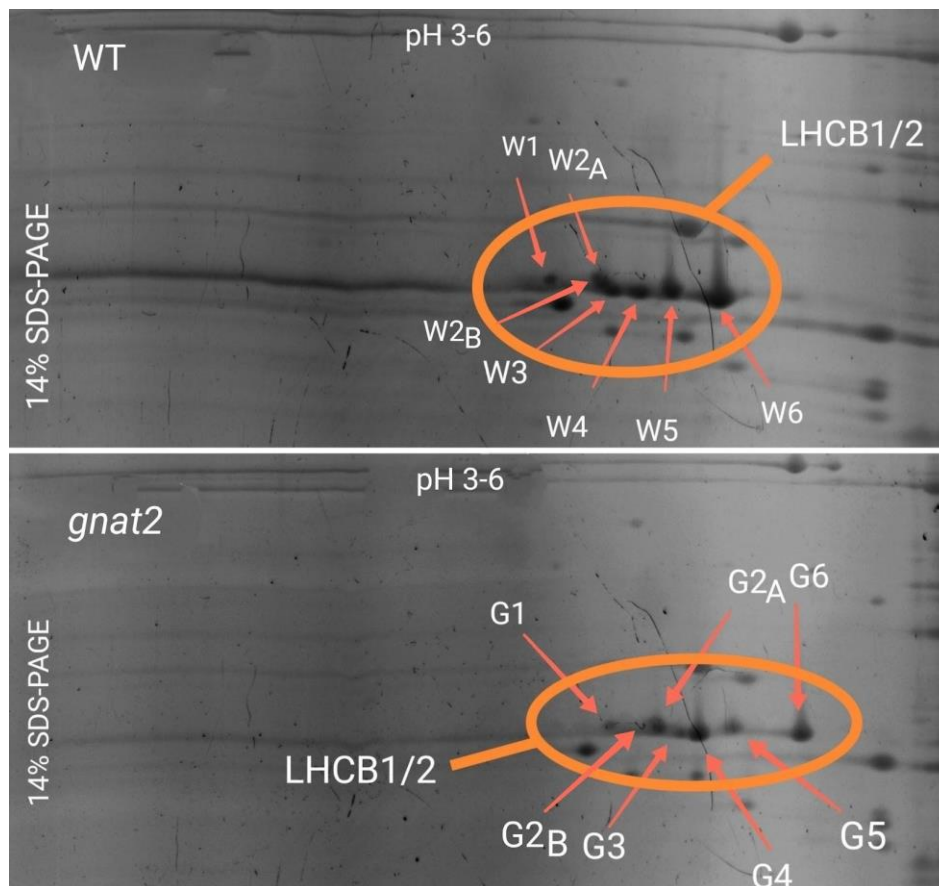


Figure 11. Magnified image of the regions of gels (Figure 10) that showed pI shift in thylakoid proteins. Isolated thylakoid proteins WT and *gnat2* plants were separated by IEF (pH 3-6) followed by 14% SDS-PAGE and SYPRO[®] staining. Spots chosen for MS analysis are indicated with arrows.

Table 1: Comparison of PTMs in WT and *gnat2* for pH 3-6 (Figure 11).

Protein	Accession number	PTM (WT)	PTM (<i>gnat2</i>)
LHCB1	P04778	Acetyl K37 K41 K43 Phospho T34 T38 S48	Acetyl K16 K37 Phospho T38 S48 T91
LHCB 2.1	Q95HR7	Acetyl K93 K120 Phospho T40	Acetyl K93 K120 K124 Phospho T40 S119
LHCB 2.2	Q95717	Acetyl K93 K120 Phospho T40	Acetyl K93 K120 K124 Phospho T40 S119
LHCB 2.4	Q9XF87	Acetyl K37 K94 K125 Phospho T38 T41	Acetyl K94 K121 Phospho T41

Table 2: Comparison of abundance (based on precursor ion area) of N-terminal peptides for each spot (on Figure 11) with and without NTA.

Protein	Peptide sequence	Spot	NTA status	Abundance WT	Abundance <i>gnat2</i>
LHCB1 (P04778)	[M].RKTVAKPKGPSG SPW.[Y]	1	+NTA	2.25e8	
			-NTA		
	[M].RKTVAKPKGPSG SPW.[Y]	2A	+NTA	1.6e9	
			-NTA		
	[M].RKTVAKPKGPSG SPW.[Y]	2B	+NTA	4.53e9	1.3e8
			-NTA		5.77e9
			+NTA	3.97e6	
			-NTA		4.07e6
	[M].RKTVAKPKGPSG SPWY.[G]	2B	+NTA	3.97e6	
			-NTA		4.07e6
			+NTA	3.97e6	
			-NTA		4.07e6
	[M].RKTVAKPKGPSG SPW.[Y]	3	+NTA	3.28e9	6.29e6
			-NTA		2.05e9
			+NTA	2.24e6	
			-NTA		
[M].RKTVAKPKGPSG SPWY.[G]	3	+NTA	2.24e6		
		-NTA			
		+NTA	2.24e6		
		-NTA			
[M].RKTVAKPKGPSG SPW.[Y]	4	+NTA	7.01e9	9.72e6	
		-NTA	9.87e6	9.11e9	
		+NTA	2.32e7		
		-NTA		1.98e7	
[M].RKTVAKPKGPSG SPWY.[G]	4	+NTA	2.32e7		
		-NTA		1.98e7	
[M].RKTVAKPKGPSG	5	+NTA	9.6e8	1.91e7	

	SPW.[Y]		-NTA	6.29e7	5.9e9
	[M].RRTVAKPKGPSG SPW.[Y]	6	+NTA	8.06e8	
			-NTA		1.44e10
LHCB2 (Q95HR7, Q95717, Q9XF87)	[M].RRTVKSTPQSIW Y.[G]	1	+NTA		3.49e6
			-NTA		
	[M].RRTVKSTPQSIW.[Y]	2A	+NTA	6.94e8	
			-NTA		9.27e8
	[M].RRTVKSTPQSIW Y.[G]		+NTA	2.78e8	
			-NTA		4.86e8
	[M].RRTVKSTPQSIW.[Y]	2B	+NTA	9.42e7	
			-NTA		1.18e8
	[M].RRTVKSTPQSIW Y.[G]		+NTA	4.93e7	
			-NTA		5.51e7
	[M].RRTVKSTPQSIW Y.[G]	3	+NTA		
			-NTA		6.1e5
	[M].RRTVKSTPQSIW.[Y]	4	+NTA		
			-NTA		6.99e6
[M].RRTVKSTPQSIW Y.[G]		+NTA			
		-NTA		3.64e6	

	[M].RRTVKSTPQSIW Y.[G]	5	+NTA	5.48e6	
			-NTA		

After the success in the pH 3-6 range, the same amount (100 μ g) of protein samples was run in the pH 5-8 range under the same conditions and treatments. The chosen staining was Coomassie R250. But presumably due to the low abundance of expected protein complexes in that pH range, the spots derived were very faint and not clear and conclusive enough for further analysis (Figure 12).

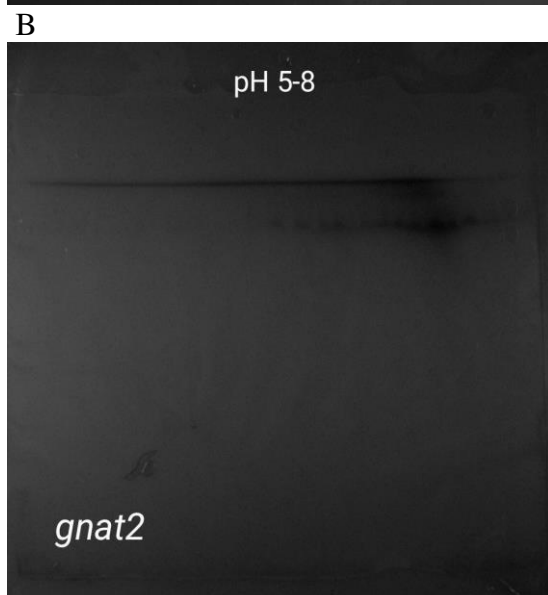
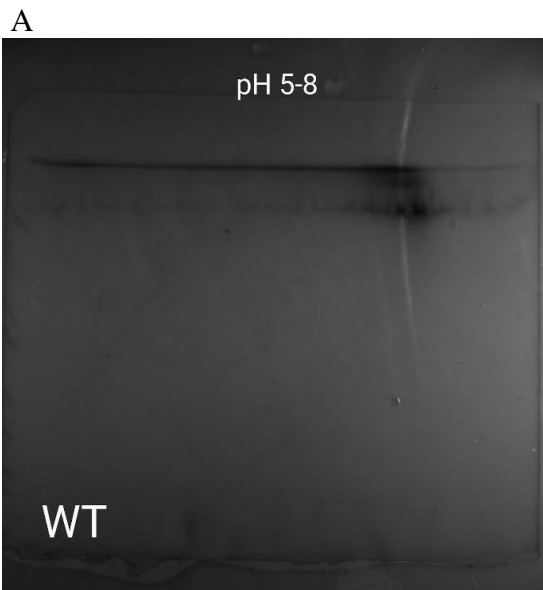


Figure 12: 2D-IEF-SDS-PAGE gel images of 100 μ g of RB treated WT (A) and *gnat2* (B) thylakoid protein complexes in pH 5-8 ranges. Coomassie R250 was applied for staining.

Hence, the next attempt was done in the same pH range with 500 μg of each sample. This time, the spots had higher visibility and showed a clear shift in pI for several spots after vertical alignment of the gel images (Figure 13).

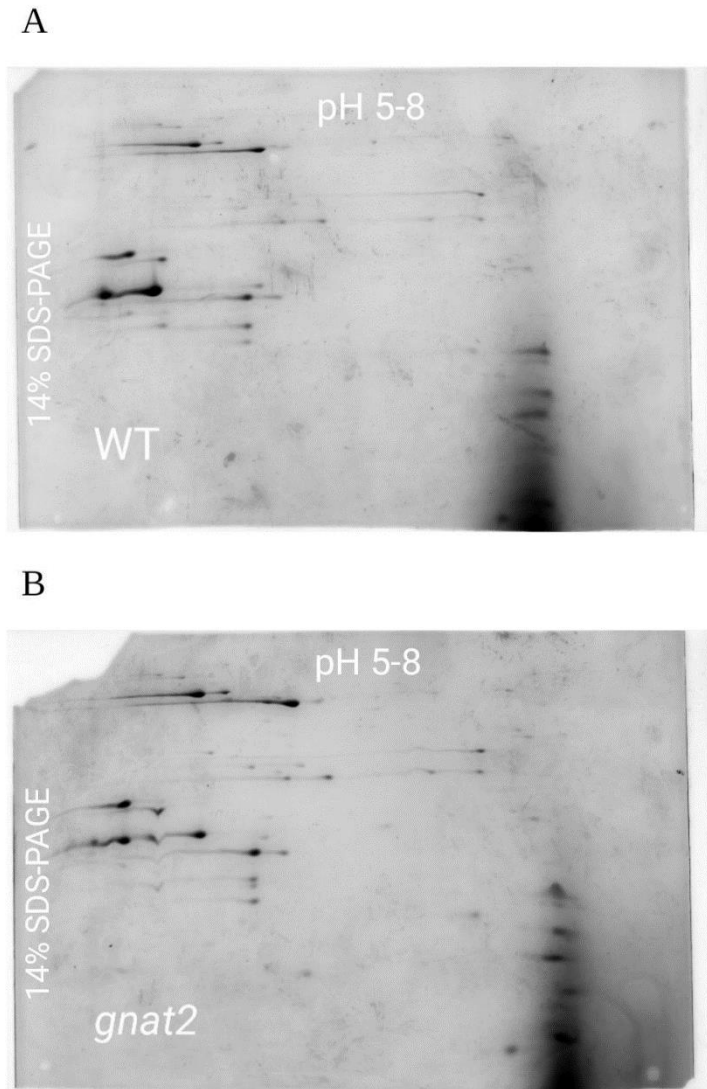


Figure 13: 2D-IEF-SDS-PAGE gel images of RB treated 500 μg WT (A) and *gnat2* (B) thylakoid protein complexes in pH 5-8 ranges followed by Coomassie R250 staining.

Based on the alignment, two spots for each gels were chosen for LC-ESI-MS/MS analysis. Each of the *gnat2* spots were further divided into two subspots, resulting in four samples in total for *gnat2*. These samples were designated as W1 and W2 for WT and G1a, G1B, G2a and G2b for *gnat2*, where each number indicates the supposedly same thylakoid complex in both WT and *gnat2* (Figure 14). As the proteins in this pH range were not presumed, the digestion enzyme used by the proteomics lab was Trypsin this time, as the default enzyme of choice. The MS analysis showed different patterns of acetylation - although there are common acetylations between WT and *gnat2*, but there were unique acetylations for both WT and *gnat2* (Table 3).

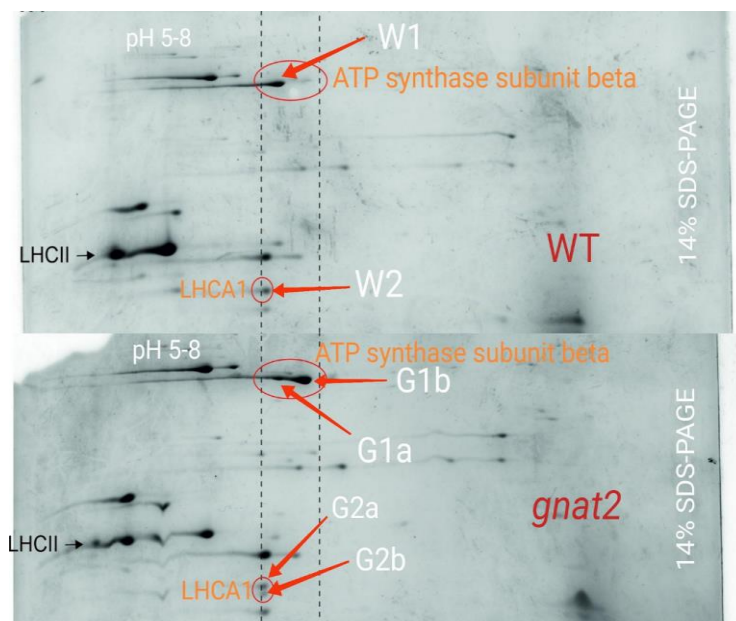


Figure 14: Magnified image of the regions of gels (Figure X) that showed pI shift in thylakoid proteins. Isolated thylakoid proteins WT and *gnat2* plants were separated by IEF (pH 3-6) followed by 14% SDS-PAGE and Coomassie R250 staining. Spots chosen for MS analysis are indicated with arrows.

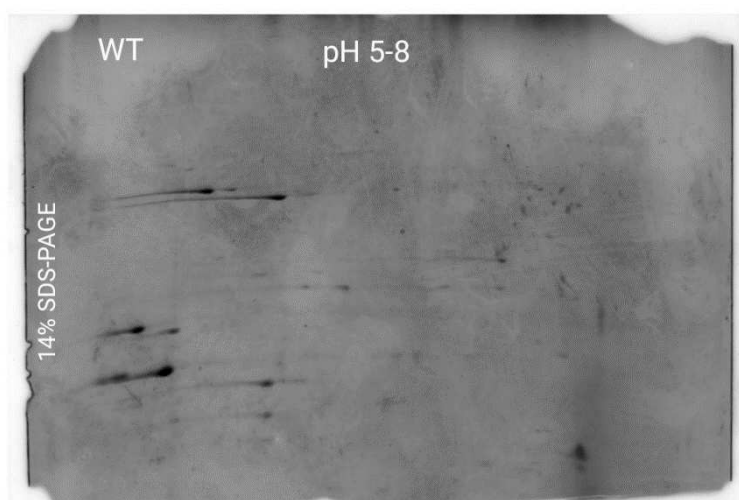
Table 3: Comparison of PTMs in WT and *gnat2* for pH 5-8 (Figure 14).

Protein	Accession number	PTM (WT)	PTM (<i>gnat2</i>)
ATP synthase subunit beta	P19366	Acetyl K39 K50 K231 K447 N-terminal Phospho S130 S135 S197 T387	Acetyl K50 K154 K217 K231 N-terminal Phospho T6 T7 S80 S197 S230 T252 T387
LHCA1	Q01667	Acetyl K179	Phospho S86 S178

		Phospho S178	
--	--	------------------------	--

Because Trypsin cleaves at the C-terminal of lysine and arginine which occupy N-terminal amino acids of the detected proteins, NTA data were missing from the LC-ESI-MS/MS report. So, the experiment was repeated, this time with the same amount of protein (500 μ g), with the goal of digesting protein complexes with chymotrypsin. But due to unidentified technical error, the results were inconsistent and thus inconclusive (Figure 15).

A



B

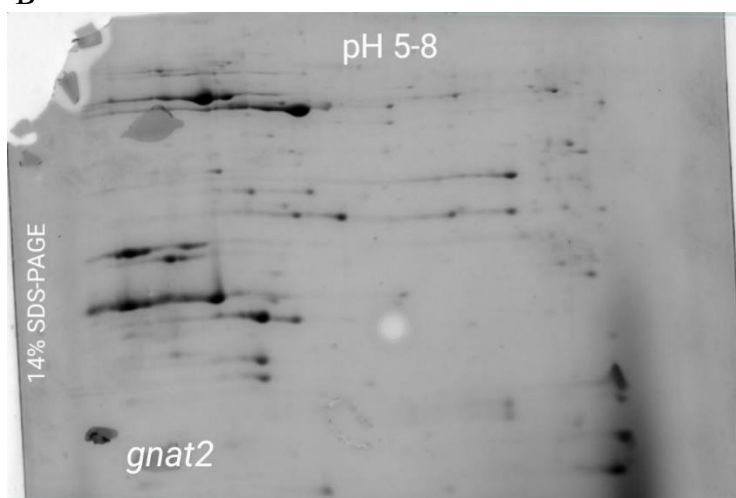


Figure 15: 2D-IEF-SDS-PAGE gel images of 500 μ g of WT (A) and *gnat2* (B) thylakoid RB treated protein complexes in pH 5-8 ranges followed by Coomassie R250 staining.

In the next round of experiments, the thylakoid samples were treated with SB buffer and DTT to enhance solubilization of light reaction center proteins. The first attempt was done in the

pH 3-6 range with an even higher amount of protein (1 mg) per sample than previous experiments followed by Coomassie R250 staining. But the experiment did not result in any significant differences compared to the first attempt in the same pH range (Figure 16).

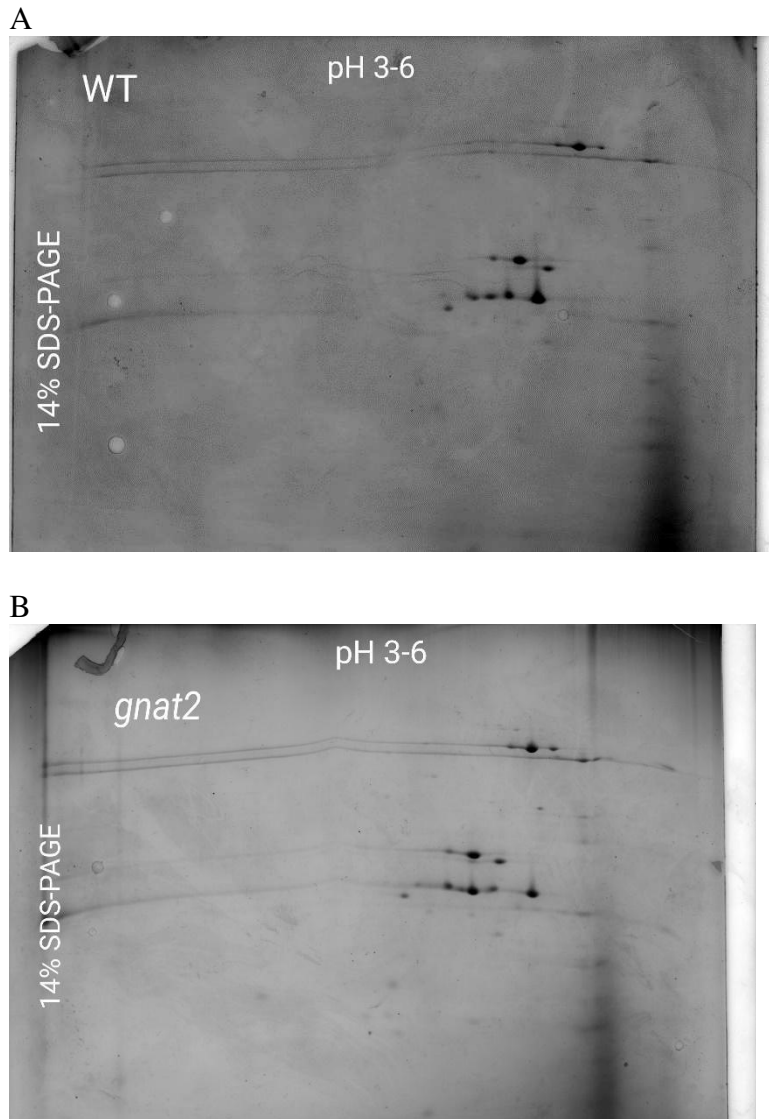


Figure 16: 2D-IEF-SDS-PAGE gel images of 1 mg of SB treated WT (A) and *gnat2* (B) thylakoid protein complexes in pH 3-6 ranges and Coomassie R250 was applied for staining. The SB treatment didn't result in any new spots compared to RB treatment.

The premise of reaction center proteins was further explored in pH 5-8 with the SB buffer. But this time, the amount of protein per sample prepared for the gel run was double the amount of the last experiment (2 mg), followed by Coomassie R250 staining. Vertical alignment of resulting gel images hinted at a few probable candidates for further analysis (Figure 17). But the high amount of protein became disadvantageous as most of the spots were somewhat overlapping due to the high abundance (Figure 17). As the spots lied toward the basic range, the further LC-ESI-MS/MS had been put on hold in the hope of getting better resolution with pH 7-10 strips.

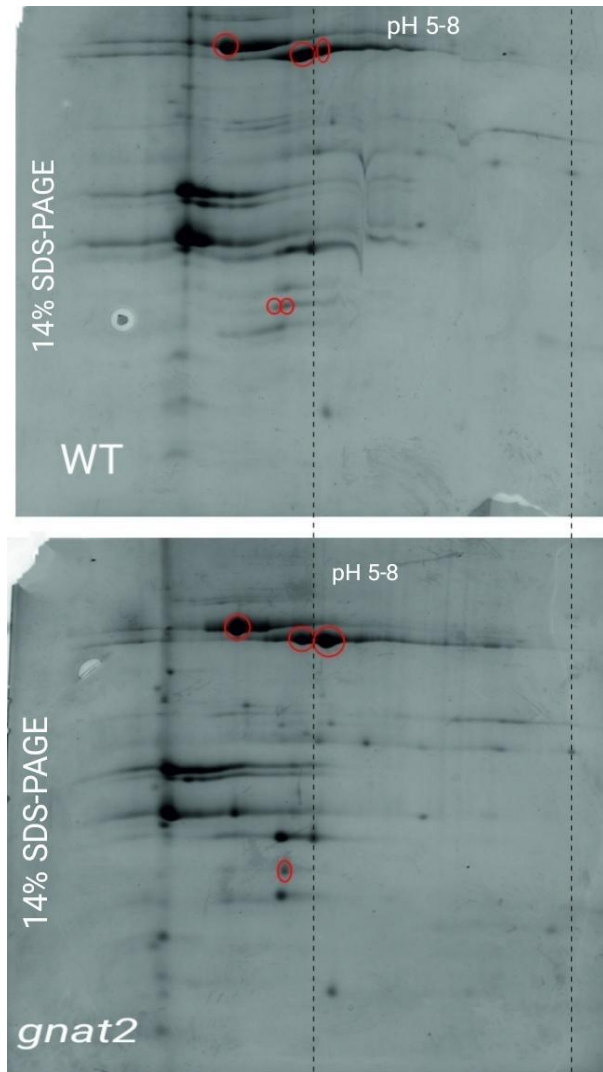


Figure 17: 2D-IEF-SDS-PAGE gel images of 2 gm of SB treated WT (A) and *gnat2* (B) thylakoid protein complexes in pH 5-8 ranges and Coomassie R250 was applied for staining. Spots show shifts in pI and are candidates for LC-ESI-MS/MS.

4.3. CN-PAGE of intact thylakoid complexes

D2 acetylation might affect the biosynthesis process of PSII. The Lys acetylation status of the D2 protein in *gnat1* and *gnat2* mutants have been shown to be decreased (Bruenje et al, unpublished). To find out the role of GNAT2 and GNAT1 in Lys-acetylation of thylakoid proteins, and further on, their role in the early stages of PSII biosynthesis, WT, *gnat1* and *gnat2* plants were cultivated for two weeks because during that time period, photosystem biosynthesis occurs. Then to separate intact thylakoid protein complexes, the thylakoid samples were subjected to CN-PAGE.

Comparison of the thylakoid protein complexes between WT, *gnat1* and *gnat2* plants indicated differences in the accumulation of PSII-LHCII supercomplexes and LHCII assembly complex (Figure 19). The PSII-LHCII band for *gnat2* appeared more intense followed by WT and *gnat1*. In the case of the LHCII assembly complex, the order of intensity

was WT, *gnat1* and *gnat2*. In order to validate the results, it was imperative to repeat the experiment with multiple biological replicates. But due to the low yield of chloroplasts isolated from the two other biological replicates, the experiment couldn't be repeated during the limited research time period.

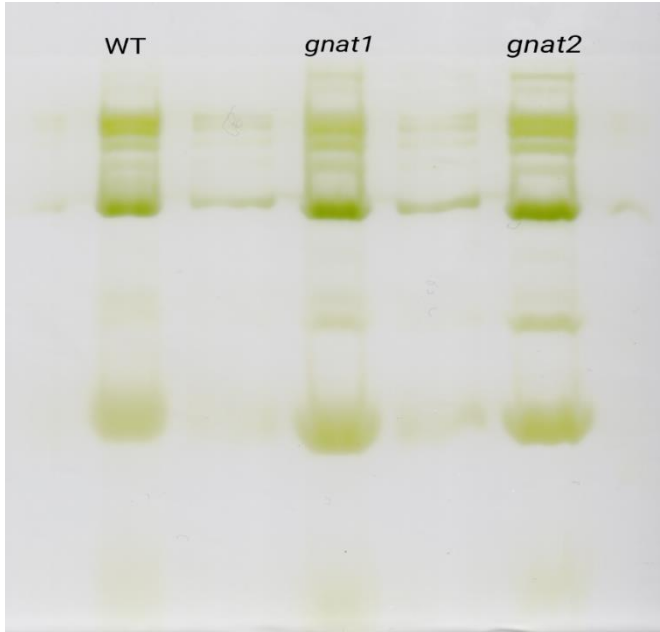


Figure 18: A digital scan of 3.5-10% gradient 0.75 mm large pore CN gel after the completion of electrophoresis. The thylakoid complex samples subjected to CN-PAGE were extracted from WT, *gnat1* and *gnat2* plants

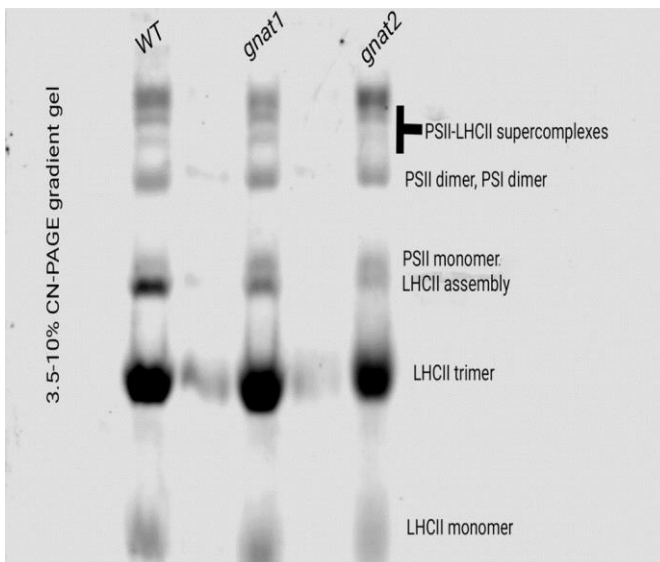


Figure 19: Analysis of thylakoid protein complexes in the WT, *gnat1* and *gnat2* plants. Thylakoid proteins were isolated and solubilized using 10% β -DM and chlorophyll protein complex samples (10 μ g) were separated using CN-PAGE. The image shows a fluorescent scan of the CN gel.

5. Discussion

5.1 The GNAT2 enzyme affects the acetylation level of the LHCb proteins.

The objective of the study was to investigate the impact of GNAT2 on chloroplast protein accumulation and NTA. In order to do so, thylakoid proteins extracted from the WT and *gnat2* mutant plants were subjected to 2D-gel electrophoresis and subsequently MS. The findings shed light on the regulatory function of GNAT2 by revealing notable variations in the pI and acetylation patterns of many thylakoid proteins (Figure 10 and 13; Table 1, 2 and 3).

Prior analyses conducted on *Arabidopsis* demonstrated the influence of GNAT2 on the acetylation of chloroplast proteins. (Bienvenuet et al. 2020). GNAT2's distinct substrate selectivity was demonstrated, but it was not possible to identify proteins embedded in thylakoids in small quantities or the abundance of NTA (Koskela et al. 2018). According to structural study, loop region alterations may be the cause of GNATs' multiple activity (Liszcak & Marmorstein, 2013). Also, the role of coupled PSII-LHCII supercomplexes in mediating plant thylakoid membrane stacking was investigated using the structural mass spectrometry (Albanese et al. 2022). The result demonstrated the interaction between the stroma-exposed N-terminal loops of LHCII trimers and the Lhcb4 subunits facing one another in neighboring membranes. The interaction allows grana to stack under varying light circumstances. The interactions between pairs of PSII-LHCII supercomplexes across the stromal gap are affected by NTA and light-dependent LHCII N-terminal trimming.

Using 2D gel electrophoresis with IEF and SDS-PAGE, then Coomassie R250 staining, I was able to reveal differences in the pI of many proteins between *gnat2* mutant and WT plants with improved resolution. The MS analysis of the six spots for each genotype (two subspots for spot 2) derived from pH 3-6 gels revealed different patterns of acetylation. Although common acetylations are shared between WT and *gnat2*, there are unique acetylations for both WT and *gnat2* (Table 1). WT showed two unique acetylations for LHCb1 (K41 and K43) and two unique acetylations for LHCb2.4 (K25 and K137). *Gnat2* showed four unique acetylations - K16 on LHCb1, K124 on LHCb2.1, K124 on LHCb2.2 and K121 on LHCb2.4. They also revealed that the NTA levels of LHCb1 and LHCb2 were decreased in the *gnat2* mutant (Table 2). In the case of LHCb1 protein, there was a higher cumulative abundance of N-terminal acetylated peptides in all spots for WT. The MS analysis of WT revealed that spot 1, 2A, 2B, 3 and 6 had only N-terminal acetylated peptides, whereas spot 4 and 5 also had non N-terminal acetylated peptides alongside their acetylated counterparts. For *gnat2*; spot 2B, 3, 4 and 5 had both N-terminal acetylated and non-acetylated peptide, whereas spot 6 had only non N-terminal acetylated peptides. In case of LHCb2 protein, there were higher cumulative abundance of N-terminal acetylated peptides for WT in spot 2A, 2B and 5; and for *gnat2* in spot 1. The MS analysis of WT revealed that spot 2A, 2B, and 5 had only N-terminal acetylated peptides. For *gnat2*; spot 2A, 2B, 3 and 4 only non-acetylated peptide; and spot 1 had only N-terminal acetylated peptides. Likewise, the LC-ESI-MS/MS analysis of 2 spots (two subspots for both spot 1 and 2 in *gnat2*) derived from pH 5-8 revealed different patterns of acetylations between WT and *gnat2*. WT showed two unique acetylations - K179 on LHCA1 (derived from spot 2) and K39 on ATP Synthase subunit beta (derived from spot1). *Gnat2* showed only one unique acetylation - K217 on ATP Synthase subunit beta (derived from spot 1A and 1B). These results discussed above imply

that acetylation patterns particular to *gnat2* may influence the function and regulation of proteins. As a result, it might change the photosynthetic efficiency and energy metabolism of the *gnat2* mutant in comparison to the WT.

The involvement of GNAT2 in the post-translational modification of thylakoid proteins is highlighted by the observed variations in protein acetylation and pI shifts between WT and *gnat2* mutants. These changes probably have an impact on the stability, function and interactions of proteins inside the chloroplast, which affects photosynthetic efficiency and plant growth, as previously shown for the organization of thylakoid protein complexes and state transition (Ivanauškaite et al. 2023; Rantala et al. 2023).

Numerous technical issues plagued the study, such as trypsin's tendency for cleaving at lysine and arginine. As the peptides possibly had those residues at the N-terminal, trypsin cleavage resulted in very small N-terminal terminal fragments which were too small in size for MS analysis. This led to NTA data missing in results for pH 5-8. That's why, future studies should consider chymotrypsin or any other enzyme which will result in MS compatible peptide fragments with intact N-terminus. Also during the course of the project, in an attempt to improve the solubilization of light reaction center proteins, the last two rounds of experiments incorporated SB buffer instead of RB and the amount of protein prepared for gel run was also increased. These changes, however, did not result in appreciable increases in resolution, and in the last attempt, high protein abundance resulted in overlapping spots, which made additional analysis more difficult. The optimization of experimental settings in order to obtain clear and replicable results is imperative for the future attempts for pH range 7-10.

Future studies should focus on optimizing experimental conditions to achieve consistent and high-resolution protein separation. This includes refining buffer compositions, adjusting protein amounts, and exploring different pH ranges for IEF. Investigating the functional consequences of altered acetylation patterns on thylakoid proteins, particularly LHCB1 and LHCB2, could elucidate the mechanisms by which GNAT2 influences photosynthesis and plant growth. Moreover, expanding the analysis to include other PTMs and their interactions with acetylation could offer a broader perspective on the regulatory networks governing chloroplast protein function.

In conclusion, this study advances our understanding of the role of GNAT2 in chloroplast protein acetylation and highlights the challenges and iterative nature of experimental optimization. The findings provide a foundation for future research aimed at uncovering the molecular mechanisms underlying GNAT2's regulatory functions and their implications for plant physiology and development.

5.2 The loss of the GNAT2 enzyme results in defects in seed germination and growth of roots under standard and osmotic stress conditions.

According to the previous studies, significant phenotypic changes are caused by deletion of GNAT2. Among them, melatonin production and photosynthetic state transitions were especially reported to be affected. WT plants respond to stress by producing more melatonin. But *gnat2* mutant plants do not exhibit this response, indicating a potential role for GNAT2 in melatonin synthesis and stress tolerance (Lee et al. 2014, Leverne et al. 2023). The absence

of the PSI-LHCII supercomplex in low to moderate light indicates that state transition in photosynthesis is perturbed in *gnat2* mutants (Koskela et al. 2018). The improper energy redistribution caused by binding incapacity of phosphorylated LHCII trimers to the PSI complex hinders the formation of this supercomplex (Kouřil et al. 2005; Koskela et al. 2018). Moreover, the significance of GNAT2 in thylakoid protein complex rearrangements and state transitions is further highlighted by the increased LHCII phosphorylation, appressed grana stacks, and negligible light-induced thylakoid dynamics observed in *gnat2* mutants (Kyle et al. 1983; Pietrzykowska et al. 2014; Koskela et al. 2018; Rantala et al. 2022).

Leverne et al. (2023) have shown that the main root of the WT was thinner and shorter compared to the *gnat2* mutants. They also demonstrated that lateral root development was strongly increased in the mutants. When plants were grown under osmotic stress conditions (200 mM mannitol), the difference between the lengths of the main root in seedlings of WT and mutants was even higher. However, visual investigation of the *gnat2* plants grown in Biocity laboratories have not supported this observation. Therefore, using WT and *gnat2* mutant plants cultivated under both standard and osmotic stress conditions, the role of GNAT2 enzyme in plant development, namely in root growth and seed germination, was examined. The findings show that these developmental processes are greatly impacted by the loss of GNAT2.

The results showed that under both standard and osmotic stress circumstances, the root length of *gnat2* mutant plants is significantly shorter than that of WT plants. The roots of *gnat2* mutant plants were consistently shorter than those of WT plants under standard conditions, both at one and two week periods. Similar patterns were seen when the plants were subjected to osmotic stress. At one and two week periods, the roots of the *gnat2* mutants were noticeably shorter than those of the WT plants. These findings are corroborated by the statistical analysis, with p-values from t-tests showing substantial variations between the genotypes in both scenarios. The findings highlight GNAT2's critical function in supporting healthy root development, most likely as a result of its participation in protein acetylation processes necessary for cell division and proliferation.

In *gnat2* mutants, germination rates were similarly negatively impacted under both standard and osmotic stress conditions. These findings were also corroborated by the statistical analysis, with p-values from t-tests showing statistically significant differences between the genotypes in both scenarios. Reduced germination rates in *gnat2* mutants emphasize the function of the enzyme in the early phases of seedling development, implying that GNAT2 is essential for plant growth. GNAT2-mediated acetylation of important proteins that control germination and early development responses to environmental cues may be the precise mechanism.

There were certain limitations to the study, mostly related to entanglement that prevented root measurement after the third week and fungal contamination under osmotic stress conditions. These problems point to the necessity for better experimental configurations, like the use of bigger plates or hydroponic systems to avoid entangling roots and more effective sterilization methods to prevent contamination.

Subsequent investigations may concentrate on clarifying the molecular pathways by which GNAT2 impacts seed germination and root growth. Genetic research could examine connections between GNAT2 and additional genes involved in growth and stress responses, while proteomic analysis could pinpoint particular acetylation targets of GNAT2. Furthermore, broadening the study to encompass additional environmental stress circumstances would offer a more comprehensive comprehension of GNAT2's function in plant resilience.

In conclusion, the notable decreases in germination rates and root length seen in *gnat2* mutants highlight the critical function of GNAT2 in plant development. These results lay the groundwork for additional research into the molecular pathways that GNAT2 regulates, which may have consequences for enhancing crop development and stress tolerance.

5.3 Both GNAT1 and GNAT2 may affect the accumulation of thylakoid protein complexes.

According to an unpublished paper by Bruenje et al., the Lys acetylation status of the D2 protein in *gnat1* and *gnat2* mutants is decreased. As the D2 protein is a prerequisite for the insertion of the D1 protein into the de novo synthesized Photosystem II complex, I wanted to clarify whether there are differences in the accumulation of thylakoid protein complexes of the two-week old *gnat1* and *gnat2* plants.

My preliminary results showed that the WT, *gnat1*, and *gnat2* plants accumulate thylakoid protein complexes differently. In particular, *gnat2* mutants exhibited the highest intensity of the PSII-LHCII supercomplex, followed by WT and *gnat1*. On the other hand, the LHCII assembly complex was highest in WT, decreased in *gnat1* mutants, and lowest in *gnat2* mutants. These findings imply that, in comparison to GNAT1, GNAT2 may have a more significant role in the formation or stabilization of the PSII-LHCII supercomplex. Elevated PSII-LHCII band intensity for *gnat2* may be the result of a compensatory mechanism or a different pathway in reaction to the D2 protein's decreased acetylation state.

The different roles that GNAT1 and GNAT2 play are further highlighted by the variations in the LHCII assembly complex. The decreased intensity of this complex in *gnat2* points to a potential defect in the assembly process, which might be brought on by changed protein-protein interactions or stability brought on by acetylation changes. On the other hand, the *gnat1* mutants' intermediate intensity suggests that GNAT1 also plays a role in this process, albeit a smaller one than GNAT2.

These results are noteworthy because they shed light on the precise functions of GNAT1 and GNAT2 in the acetylation of thylakoids and PSII biosynthesis. However, one significant restriction is that the limited yield of chloroplasts from additional samples prevented the experiment from being repeated with several biological replicates. This limitation emphasizes the need for additional verification of these findings in order to confirm the repeatability and dependability of the noted patterns.

The different build-up of PSII-LHCII supercomplex and LHCII assembly complexes in WT, *gnat1*, and *gnat2* plants, in summary, emphasizes the diverse but complementary functions of GNAT1 and GNAT2 in thylakoid protein acetylation and PSII production. These first results open the door to more thorough investigations to clarify the precise molecular

mechanisms behind these activities. For future studies, extending the analysis to include associated PTMs could provide a more comprehensive understanding of the regulatory mechanisms involved. Investigating the potential compensatory pathways activated in the absence of GNAT1 and GNAT2 might also uncover new aspects of photosystem regulation and assembly.

6. Conclusions

Critical understanding of GNAT enzymes and their diverse functions in plant biology has been provided by research on these enzymes. These enzymes are known to mediate protein acetylation and have a substantial impact on a number of physiological processes in plants. Clarifying the distinct roles of GNAT1 and GNAT2, especially in connection to the LHCI and LHCII proteins as well as plant development under various circumstances, has been the main goal of our research.

The results obtained so far indicate that:

- 1) The GNAT2 enzyme affects the acetylation level of the Light Harvesting Complex II proteins LHCB1, LHCB2.2, LHCB2.3 and LHCB2.4.
- 2) The loss of the GNAT2 enzyme results in defects in seed germination and growth of roots under standard and osmotic stress conditions.
- 3) Both GNAT1 and GNAT2 may affect the accumulation of thylakoid protein complexes.

The results, taken together, offer strong evidence that GNAT2 and possibly GNAT1 play in plant development and stress responses. For effective photosynthesis, LHCII protein acetylation is required, and GNAT2 is required for this process. Its significance for plant growth is further shown by its function in seed germination and root development. Furthermore, the impacts of GNAT2 on the biosynthesis of thylakoid protein complexes suggests their wider importance in preserving chloroplast function. Subsequent investigations ought to focus on deciphering the intricate molecular mechanisms that oversee these procedures and investigating their possible uses in augmenting crop resilience and production. Gaining insight into the complex roles played by GNATs may open doors for creative approaches in agricultural biotechnology. And these approaches hold the key to improve food security in the face of shifting environmental circumstances.

7. References

- Albanese, P., Tamara, S., Saracco, G., Scheltema, R. A., & Pagliano, C. (2020). How paired PSII–LHCII supercomplexes mediate the stacking of plant thylakoid membranes unveiled by structural mass-spectrometry. *Nature Communications*, *11*(1).
- Allfrey, V. G., Faulkner, R., and Mirsky, A. E. (1964). Acetylation and methylation of histones and their possible role in the regulation of RNA synthesis. *Proceedings of the National Academy of Sciences*, *51*(5), 786–794.
- Allis, C. D., Berger, S. L., Cote, J., Dent, S., Jenuwien, T., Kouzarides, T., Pillus, L., Reinberg, D., Shi, Y., Shiekhhattar, R., Shilatifard, A., Workman, J., and Zhang, Y. (2007). New nomenclature for chromatin-modifying enzymes. *Cell*, *131*(4), 633–636.
- Arnesen, T. (2011). Towards a functional understanding of protein NTA. *PLoS Biology*, *9*(5).
- Behnia, R., Panic, B., Whyte, J. R. C., and Munro, S. (2004). Targeting of the Arf-like GTPase Arl3p to the Golgi requires NTA and the membrane protein Sys1p. *Nature Cell Biology*, *6*(5), 405–413.
- Bienvenuet, W. V., Espagne, C., Martinez, A., Majeran, W., Valot, B., Zivy, M., Vallon, O., Adam, Z., Meinnel, T., and Giglione, C. (2011). Dynamics of post-translational modifications and protein stability in the stroma of *Chlamydomonas reinhardtii* chloroplasts. *Proteomics*, *11*(9), 1734–1750.
- Bienvenuet, W. V., Brünje, A., Boyer, J., Mühlenbeck, J. S., Bernal, G., Lassowskat, I., Dian, C., Linster, E., Dinh, T. V., Koskela, M. M., Jung, V., Seidel, J., Schyrba, L. K., Ivanauskaite, A., Eirich, J., Hell, R., Schwarzer, D., Mulo, P., Wirtz, Meinnel, T., Giglione, C., Finkemeier, I. (2020). Dual lysine and N-terminal acetyltransferases reveal the complexity underpinning protein acetylation. *Molecular Systems Biology*, *16*(7).
- Choudhary, C., Kumar, C., Gnad, F., Nielsen, M. L., Rehman, M., Walther, T. C., Olsen, J. V., and Mann, M. (2009). Lysine acetylation targets protein complexes and co-regulates major cellular functions. *Science*, *325*(5942), 834–840.
- Döring, G., Renger, G., Vater, J., and Witt, H. T. (1969). Properties of the photoactive chlorophyll-a_{II} in photosynthesis. *Zeitschrift Für Naturforschung B*, *24*(9), 1139–1143.
- Drazic, A., Myklebust, L. M., Ree, R., and Arnesen, T. (2016). The world of protein acetylation. *Biochimica Et Biophysica Acta (BBA)*, *1864*(10), 1372–1401.
- Eberharter, A., and Becker, P. B. (2002). Histone acetylation: a switch between repressive and permissive chromatin. *EMBO Reports*, *3*(3), 224–229.
- Forte, G. M. A., Pool, M. R., and Stirling, C. J. (2011). NTA inhibits protein targeting to the endoplasmic reticulum. *PLoS Biology*, *9*(5), e1001073.

Friedmann, D. R., and Marmorstein, R. (2013). Structure and mechanism of non-histone protein acetyltransferase enzymes. *The FEBS Journal*, 280(22), 5570–5581.

Gao, X., Hong, H., Li, W., Yang, L., Huang, J., Xiao, Y., Chen, X., and Chen, G. (2016). Downregulation of rubisco activity by non-enzymatic acetylation of RBCL. *Molecular Plant*, 9(7), 1018–1027.

Hoshiyasu, S., Kohzuma, K., Yoshida, K., Fujiwara, M., Fukao, Y., Yokota, A., and Akashi, K. (2013). Potential involvement of NTA in the quantitative regulation of the ϵ subunit of chloroplast ATP synthase under drought stress. *Bioscience, Biotechnology, and Biochemistry*, 77(5), 998–1007.

Huber, M., Bienvenut, W. V., Linster, E., Stephan, I., Armbruster, L., Sticht, C., Layer, D. C., Lapouge, K., Meinnel, T., Sinning, I., Giglione, C., Hell, R., and Wirtz, M. (2019). NatB-mediated NTA affects growth and biotic stress responses. *Plant Physiology*, 182(2), 792–806.

Ivanauskaite, A. (2023) Chloroplast protein acetyltransferases –novel players in the regulation of photosynthesis. Turun yliopiston julkaisu – Annales Universitatis Turkuensis. Sarja-Ser. AI-osa Tom. 697. Astronomica-Chemica-Physica_Mathematica. Turku.

Ivanauskaite A., Rantala M., Laihonon L., Konert M.M., Schwenner N., Mühlenbeck J., Finkemeier I. and Mulo P. Loss of chloroplast GNAT acetyltransferases results in distinct metabolic phenotypes in *Arabidopsis*. *Plant and Cell Physiology*, 2023; 64: 549-563.

Johnson, V. M., and Pakrasi, H. B. (2022). Advances in the understanding of the lifecycle of Photosystem II. *Microorganisms*, 10(5), 836.

Kok, B. (1959). Light induced absorption changes in photosynthetic organisms. II. A split-beam difference spectrophotometer. *Plant Physiology*, 34(3), 184–192.

Koskela, M. M., Brünje, A., Ivanauskaite, A., Grabsztunowicz, M., Lassowskat, I., Neumann, U., Dinh, T. V., Sindlinger, J., Schwarzer, D., Wirtz, M., Tyystjärvi, E., Finkemeier, I., and Mulo, P. (2018). Chloroplast acetyltransferase NSI is required for state transitions in *Arabidopsis thaliana*. *The Plant Cell*, 30(8), 1695–1709.

Koutelou, E., Farria, A. T., and Dent, S. Y. (2021). Complex functions of Gcn5 and Pcaf in development and disease. *Biochimica Et Biophysica Acta. Gene Regulatory Mechanisms*, 1864(2), 194609.

Kouřil, R., Zygadlo, A., Arteni, A. A., De Wit, C. D., Dekker, J. P., Jensen, P. E., Scheller, H. V., and Boekema, E. J. (2005). Structural characterization of a complex of photosystem I and light harvesting complex II of *Arabidopsis thaliana*. *Biochemistry*, 44(33), 10935–10940.

Kyle, D. J., Staehelin, L. A., and Arntzen, C. J. (1983). Lateral mobility of the light-harvesting complex in chloroplast membranes controls excitation energy distribution in higher plants. *Archives of Biochemistry and Biophysics*, 222(2), 527–541.

Lee, H. Y., and Back, K. (2018). Melatonin induction and its role in high light stress tolerance in *Arabidopsis thaliana*. *Journal of Pineal Research*, 65(3), 1–13.

Lee, H. Y., Byeon, Y., Lee, K., Lee, H. J., and Back, K. (2014). Cloning of *Arabidopsis* serotonin N-acetyltransferase and its role with caffeic acid O-methyltransferase in the biosynthesis of melatonin in vitro despite their different subcellular localizations. *Journal of Pineal Research*, 57(4), 418–426.

Lehtimäki, N., Koskela, M.M. and Mulo, P. (2015) Posttranslational modifications of chloroplast proteins: an emerging field. *Plant Physiology*, 168(3), 768–775.

Leverne, L., Roach, T., Perreau, F., Maignan, F., and Liskay, A. (2023). Increased drought resistance in state transition mutants is linked to modified plastoquinone pool redox state. *Plant Cell Environ* , 46(12), 3737-3747.

Linster, E., Stephan, I., Bienvenut, W. V., Maple-Grødem, J., Myklebust, L. M., Huber, M., Reichelt, M., Sticht, C., Møller, S. G., Meinnel, T., Arnesen, T., Giglione, C., Hell, R., and Wirtz, M. (2015). Downregulation of NTA triggers ABA-mediated drought responses in *Arabidopsis*. *Nature Communications*, 6(1).

Linster, E., and Wirtz, M. (2018). NTA: An essential protein modification emerges as an important regulator of stress responses. *Journal of Experimental Botany*, 69(19), 4555–4568.

Liszcak, G., Goldberg, J. M., Foyn, H., Petersson, E. J., Arnesen, T., and Marmorstein, R. (2013). Molecular basis for NTA by the heterodimeric NatA complex. *Nature Structural and Molecular Biology*, 20(9), 1098–1105.

Liszcak, G., and Marmorstein, R. (2013). Implications for the evolution of eukaryotic amino-terminal acetyltransferase (NAT) enzymes from the structure of an archaeal ortholog. *Proceedings of the National Academy of Sciences of the United States of America*, 110(36), 14652–14657.

Longo, C., Lepri, A., Paciolla, A., Messori, A., De Vita, D., Di Patti, M. C. B., Amadei, M., Madia, V. N., Ialongo, D., Di Santo, R., Costi, R., and Vittorioso, P. (2022). New inhibitors of the human p300/CBP acetyltransferase are selectively active against the *Arabidopsis* HAC Proteins. *International Journal of Molecular Sciences*, 23(18),

Mukherjee, S., Keitany, G., Li, Y., Wang, Y., Ball, H. L., Goldsmith, E. J., and Orth, K. (2006). *Yersinia* YopJ acetylates and inhibits kinase activation by blocking phosphorylation. *Science*, 312(5777), 1211–1214.

Müh, F., and Zouni, A., (2020). Structural basis of light-harvesting in the photosystem II core complex, *Protein Science*, 29(5), 1090–1119. .

Nickelsen, J., and Rengstl, B. (2013). Photosystem II assembly: From cyanobacteria to plants. *Annual Review of Plant Biology*, 64(1), 609–635.

Pesaresi, P., Gardner, N. A., Masiero, S., Dietzmann, A., Eichacker, L., Wickner, R., Salamini, F., and Leister, D. (2003). Cytoplasmic N-Terminal protein acetylation is required for efficient photosynthesis in *Arabidopsis*. *Plant Cell*, 15(8), 1817–1832

Peserico, A., and Simone, C. (2011). Physical and functional HAT/HDAC interplay regulates protein acetylation balance (2011). *Journal of Biomedicine and Biotechnology*, 1–10.

Peterson, C. L., and Laniel, M. (2004). Histones and histone modifications. *CB/Current Biology*, 14(14), 546–551.

Pietrzykowska, M., Suorsa, M., Semchonok, D. A., Tikkanen, M., Boekema, E. J., Aro, E. M., and Jansson, S. (2014). The light-harvesting chlorophyll a/b binding proteins Lhcb1 and Lhcb2 play complementary roles during state transitions in *Arabidopsis*. *The Plant Cell*, 26(9), 3646–3660.

Polevoda, B. (1999). Identification and specificities of N-terminal acetyltransferases from *Saccharomyces cerevisiae*. *The EMBO Journal*, 18(21), 6155–6168.

Požoga, M., Armbruster, L., and Wirtz, M. (2022). From nucleus to membrane: A subcellular map of the N-acetylation machinery in plants. *International Journal of Molecular Sciences*, 23(22), 14492.

Rantala, M., Ivanauskaite, A., Laihonon, L., Kanna, S. D., Ughy, B., and Mulo, P. (2022). Chloroplast acetyltransferase GNAT2 is involved in the organization and dynamics of thylakoid structure. *Plant and Cell Physiology*, 63(9), 1205–1214.

Scott, D. C., Monda, J. K., Bennett, E. J., Harper, J. W., and Schulman, B. A. (2011). NTA acts as an avidity enhancer within an interconnected multiprotein complex. *Science*, 334(6056), 674–678.

Smith, S., and Stillman, B. (1991). Stepwise assembly of chromatin during DNA replication in vitro. *EMBO Journal*, 10(4), 971–980.

Starheim, K. K., Gevaert, K., and Arnesen, T. (2012). Protein N-terminal acetyltransferases: When the start matters. *Trends in Biochemical Sciences*, 37(4), 152–161.

Thompson, P. R., Wang, D., Wang, L., Fulco, M., Pediconi, N., Zhang, D., An, W., Ge, Q., Roeder, R. G., Wong, J., Levrero, M., Sartorelli, V., Cotter, R. J., and Cole, P. A. (2004).

Regulation of the p300 HAT domain via a novel activation loop. *Nature Structural and Molecular Biology*, 11(4), 308–315.

Utley, R. T., and Côté, J. (2003). The MYST family of histone acetyltransferases. *In Current topics in microbiology and immunology*, 203–236.

Van Damme, P., Evjenth, R., Foyn, H., Demeyer, K., De Bock, P.-J., Lillehaug, J. R., Vandekerckhove, J., Arnesen, T., and Gevaert, K. (2011). Proteome-derived peptide libraries allow detailed analysis of the substrate specificities of N^α-acetyltransferases and point to hNaa10p as the post-translational actin N^α-acetyltransferase. *Molecular and Cellular Proteomics*, 10(5).

Varland, S., Osberg, C., and Arnesen, T. (2015). N-terminal modifications of cellular proteins: The enzymes involved, their substrate specificities and biological effects. *PROTEOMICS*, 15(14), 2385–2401.

Yang, X. (2004). The diverse superfamily of lysine acetyltransferases and their roles in leukemia and other diseases. *Nucleic Acids Research*, 32(3), 959–976.

Ye, J., Ai, X., Eugeni, E. E., Zhang, L., Carpenter, L. R., Jelinek, M. A., Freitas, M. A., and Parthun, M. R. (2005). Histone H4 lysine 91 acetylation. *Molecular Cell*, 18(1), 123–130.

Yuan, H., Rossetto, D., Mellert, H., Dang, W., Srinivasan, M., Johnson, J., Hodawadkar, S., Ding, E. C., Speicher, K., Abshiru, N., Perry, R., Wu, J., Yang, C., Zheng, Y. G., Speicher, D. W., Thibault, P., Verreault, A., Johnson, F. B., Berger, S. L., Sternglanz, R., McMahon, S.B., Côte, J. and Marmorstein, R. (2011). MYST protein acetyltransferase activity requires active site lysine autoacetylation. *EMBO Journal*, 31(1), 58–70.

Zybaïlov, B. L., Rutschow, H., Friso, G., Rudella, A., Emanuelsson, O., Sun, Q., and Van Wijk, K. J. (2008). Sorting signals, N-Terminal modifications and abundance of the chloroplast proteome. *PloS One*, 3(4), e1994.